Review

Heterobinuclear Metallocomplexes as Photocatalysts in Organic Synthesis

Violetta A. Ionova [1], Anton S. Abel [1,*], Alexei D. Averin [1] and Irina P. Beletskaya [1,2,*]

1   Department of Chemistry, Lomonosov Moscow State University, Leninskie Gory 1-3, Moscow 119991, Russia; v-ionova@mail.ru (V.A.I.); alexaveron@yandex.ru (A.D.A.)
2   Frumkin Institute of Physical Chemistry and Electrochemistry, Russian Academy of Sciences, Leninsky Pr. 31, Moscow 119071, Russia
*   Correspondence: antonabel@list.ru (A.S.A.); beletska@org.chem.msu.ru (I.P.B.)

Abstract: Photocatalytic processes under visible light have constantly been finding more and more applications in organic synthesis as they allow a wide range of transformations to proceed under mild conditions. The combination of photoredox catalysis with metal complex catalysis gives an opportunity to employ the advantages of these two methodologies. Covalent bonding of photocatalyst and metal complex catalyst using bridging ligands increases the efficiency of the electron and energy transfer between these two parts of the catalyst, leading to more efficient and selective catalytic systems. Up to now, after numerous investigations of the photocatalytic reduction of CO_2 and hydrogen generation, such a strategy was firmly established to substantially increase the catalyst's activity. This review is aimed at the achievements and perspectives in the field of design and application of heterobinuclear metal complexes as photocatalysts in organic synthesis.

Keywords: binuclear complexes; photocatalysis; supramolecular catalysts; metallaphotoredox catalysis; cross coupling; metal complexes

1. Introduction

The 21st Century witnessed the active introduction of photoredox catalysis in synthetic chemistry using visible light (400–700 nm); this trend provided new possibilities to the organic chemistry of free radicals [1,2]. A wide range of available photocatalysts with different RedOx potentials in ground and excited states allows the selective and efficient generation of free radicals under the action of visible light. It opens the way to various reactions, from simple processes such as aerobic oxidation of amines, thiols and alcohols, to multi-component processes such as radical arylation, cycloaddition, halogenation, di-functionalization of alkenes, etc. [3–6]. New synthetic approaches to a great variety of molecules, including sophisticated natural compounds, are provided [7].

In recent years, metallaphotoredox catalysis, which employs mutual application of the photoredox catalysis and catalysis with transition metal complexes under the action of visible light [8,9], has been actively developed. This allows us to combine mild reaction conditions and visible light as the energy source (main features of the photoredox catalysis) with the key advantages of transition metal catalysis such as chemo-, regio- and enantioselectivity [9–11].

There are many examples of metal-catalyzed reactions which proceed under visible light irradiation [12], with the intermediate complex in the excited state, which favors the reductive elimination step. Often the ability of such complexes to absorb visible light is insufficient, and the use of high-energy ultraviolet irradiation may lead to undesirable side photochemical reactions. Due to the application of photoactive Ru(II) or Ir(III) complexes [7,13] or dyes, such as Eosin Y and BODIPY [6], which are characterized by high molar extinction coefficients in the range of 400–600 nm, metallaphotoredox catalytic reactions can be performed under visible light irradiation. Significant progress in this field

has occurred due to the use of various inorganic conductors (TiO_2, CdS, MoS_2, quantum dots, C_3N_4, etc.) as photocatalysts [14–17]. Varying their structure and doping with various components provides high activity in various photocatalyzed redox processes. Moreover, being heterogeneous, these catalysts can be separated from the reaction mixture and reused, as well as used in flow reactors [18,19].

Metal complexes as components of the metallaphotoredox catalytic systems usually incorporate nickel, copper, palladium and gold, and in rare cases, cobalt and some other metals [9]. A key step in the catalytic transformations with such systems is a single electron transfer (SET) or energy transfer (EnT) between photocatalytic and metal complex parts. It is quite logical to ensure the covalent binding of these two components using bridging ligands whose structure should provide their best synergism (Scheme 1).
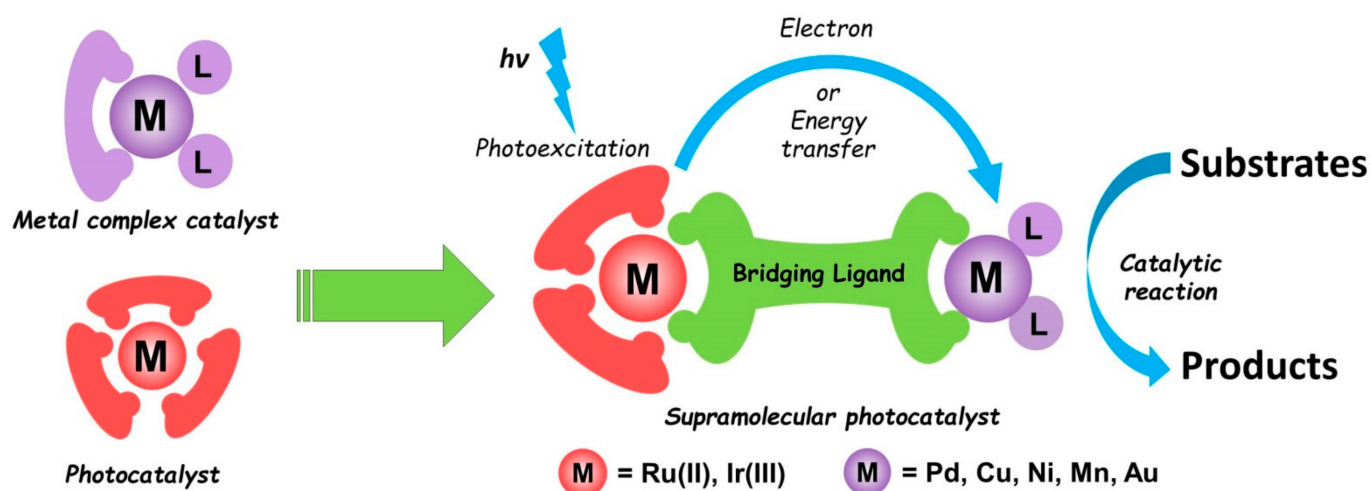
Scheme 1. Schematic diagram of covalently bonded photocatalyst.

To date, energy and electron transfer processes in di- and polynuclear complexes have been extensively studied using various spectral and electrochemical methods, as well as DFT calculations [20–28], allowing us to find out appropriate complexes for catalytic purposes. During the last two decades, great progress was achieved in the application of supramolecular catalysts in the CO_2 photoreduction [29–31] and hydrogen photogeneration [32–34], which is helpful for the fine-tuning of the catalytic properties of binuclear complexes. As for metallaphotoredox catalysis, it has been rapidly developing during the last 7 years, and the application of binuclear complexes is still limited. In the present review, we address known examples of heterobinuclear metallocomplexes as photocatalysts in order to demonstrate the challenges and perspectives of their use in organic synthesis.

2. Heterobinuclear Photocatalysts

As our main interest is the application of heterobinuclear photoactive metal complexes in the synthesis of organic compounds, their use in the photocatalytic CO_2 reduction [29–31] and hydrogen photogeneration [32–34] could be judged to be beyond the frames of this review. Moreover, each of these reactions was dealt with in excellent reviews covering achievements and tendencies in this field. However, the efficiency of the covalent bonding of the photoactive Ru(II) or Ir(III) complex with the catalytic metallocomplex center was first described for these processes. In the frames of these reactions, various photophysical and physicochemical studies of electron and energy transfer were carried out, and the main synthetic approaches to the polyazine heterobinuclear complexes were elaborated. As a result, the rapid development of the use of such complexes in organic synthesis was strongly supported by these investigations. Thus, we suppose to consider selected catalytic systems employed in the photocatalytic CO_2 reduction and hydrogen photogeneration to

underline a great variety of known bridging ligands and supramolecular photocatalysts and to show the possibilities of their adjustment to a certain catalytic process.

Classical ditopic polyazine ligands are given in Figure 1; they differ by the conjugation between two coordination sites, flexibility, and distance between metallocenters.
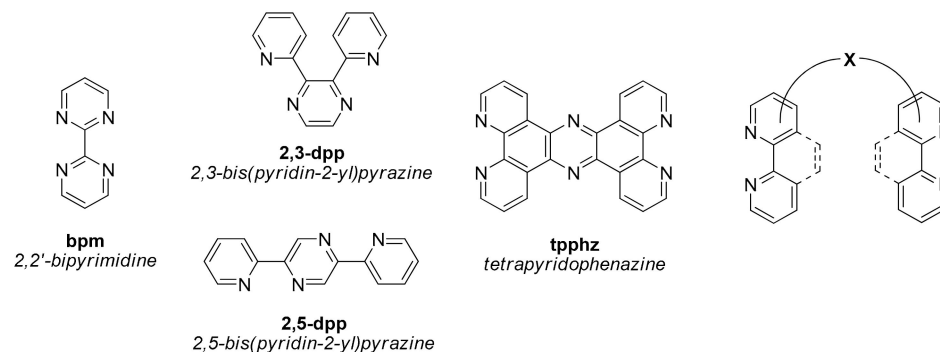

bpm
2,2'-bipyrimidine

2,3-dpp
2,3-bis(pyridin-2-yl)pyrazine

2,5-dpp
2,5-bis(pyridin-2-yl)pyrazine

tpphz
tetrapyridophenazine

Figure 1. Commonly used polyazine bridging ligands.

2.1. Heteropolynuclear Complexes for Hydrogen Photogeneration

Hydrogen is considered to be one of the most important ecologically clean sources of energy, which is to become a key component in the transition to "green" energetics and sustainable development. The use of solar light is one of the techniques to produce environmentally friendly hydrogen, and this fact stimulates the search for hydrogen photogeneration catalysts. Photocatalyst absorbs visible light assuring its transition to an excited state and provides the electron transfer to the metal complex catalyst (usually Pd, Pt or Rh). Ru(II) polypyridine complexes are thought to be most perspective as photoactive components as they possess a unique combination of spectral, photophysical and electrochemical properties [35]. The transfer of two electrons from the photocatalyst to the metal catalytic center provides the formation of one molecule of dihydrogen. Creating favorable conditions for the electron transfer process is a way to increase the efficiency of the catalytic system [34]. Triethylamine is used as a reductant, and the reactions are carried out in acetonitrile-water media.

The general mechanism of hydrogen photogeneration catalyzed by the Ru-Pd binuclear complex is depicted in Scheme 2. Under visible light irradiation, the electron is promoted from Ru(II)-center to π*-orbitals of the bridging ligand (Metal Ligand Charge Transfer, MLCT). Then, Ru(III) accepts the electron from the sacrificial reductant (triethylamine), followed by the electron transfer from the bridging ligand to Pd(II) and proton reduction [34].
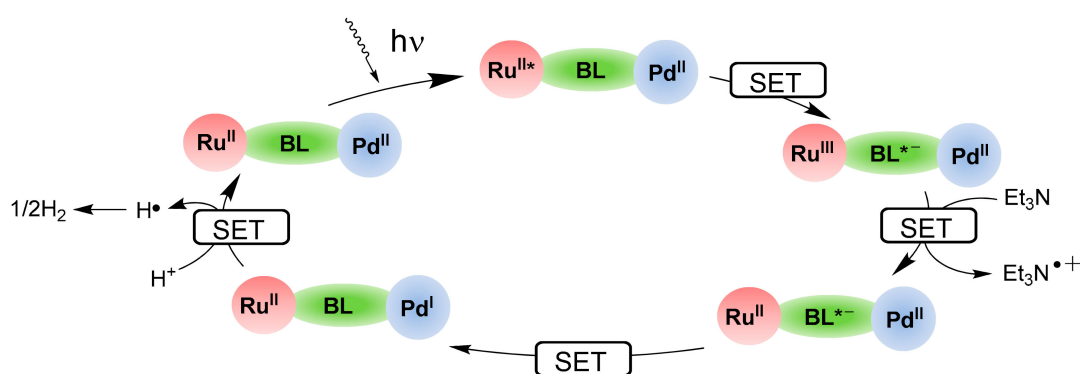
Scheme 2. General mechanism of hydrogen photogeneration [34]. BL–bridging ligand.

The main characteristic showing the activity and robustness of the catalyst is its TON. Recently, it has been shown [36] that even a simple spatial approach of the photoactive and

catalytic components using supramolecular interactions of the type "host–guest" increases the efficiency of the catalyst in this process. Covalent bonding of the photocatalyst with the metal catalytic center provides a further increase in the catalyst activity [33,34]; nowadays, a good number of such catalytic systems have been reported [37]. During the last 15 years, extended studies of bi- and polynuclear complexes were conducted, demonstrating the efficiency of this strategy [32–34]. The most representative examples will be discussed below.

Systematic theoretical and experimental investigation of Ru-Pd and Ru-Pt binuclear complexes in the photogeneration of dihydrogen is described in the papers by Vos and Rau. The studies reported in [38–41] dealt with binuclear complexes for hydrogen production with 2,5-bis(pyridin-2-yl)pyrazine (**RuPd-1** and **RuPd-2**), 2,2′:5′,2″-terpyridine (**RuPd-3**, **RuPt-1** and **RuPt-2**) and 2,2′:6′,2″-terpyridine (**RuPd-4**) as bridging ligands (Figure 2). It was revealed that the **RuPd-1** complex was not catalytically active, and only the presence of electron-withdrawing substituents in the **RuPd-2** complex allowed TON 400 in 18 h. Among the cyclometallated complexes **RuPd-3** and **RuPd-4,** only the first one was catalytically active (TON 138, lower than for the **RuPd-2** complex). To note, during the first 8 h its TON was higher than that found for the mixed catalytic systems (Ru-complex/Pd(MeCN)$_2$Cl$_2$). Platinum complexes **RuPt-1** and **RuPt-2** with TONs 80 and 650, respectively, turned out to be more reactive than corresponding Ru-Pd complexes.
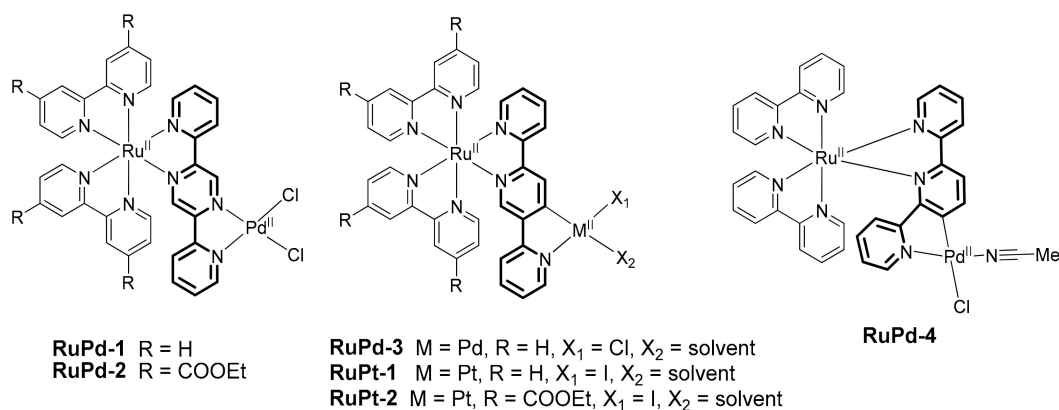

RuPd-1 R = H
RuPd-2 R = COOEt

RuPd-3 M = Pd, R = H, X$_1$ = Cl, X$_2$ = solvent
RuPt-1 M = Pt, R = H, X$_1$ = I, X$_2$ = solvent
RuPt-2 M = Pt, R = COOEt, X$_1$ = I, X$_2$ = solvent

RuPd-4

Figure 2. Ru-Pd and Ru-Pt complexes with 2,5-bis(pyridin-2-yl)pyrazine or 2,2′:5′,2″-terpyridine for hydrogen photogeneration.

Pt complexes **RuPt-3** and **RuPt-4** with 2,3-bis(pyridin-2-yl)pyrazine as a bridging ligand (Figure 3) were inefficient as catalysts of hydrogen generation, and only **RuPt-5** provided TON 44 for 18 h [42].

Brewer and coworkers studied **RuRh-1**–**RuRh-4** complexes (Figure 3) with Rh(III) in the catalytic center. **RuRh-2**, containing terpyridine as a peripheral ligand, demonstrated better activity in DMF than **RuRh-1** complex with 2,2′-bipyridines (TONs 58 and 33, respectively) [43]. Studying the trinuclear complexes of **RuRh-3** type (Figure 3) revealed that the hydroxo complex was the most active in DMF [44]. Further development of the catalysts of this type led to a water-soluble complex **RuRh-4** with sulfo groups, which provided TON 120 for 18 h in an aquatic medium with the ascorbate buffer [45].

The same researchers studied Ru-Pt complexes **RuPt-6**–**RuPt-8** (Figure 4) [46]. The authors explored the influence of π-extended bridging ligands and the increased number of photoactive centers in the structure of supramolecular catalysts on their efficiency. **RuPt-8** complex comprising three photoactive Ru(II) centers was shown to be less efficient than the **RuPt-7** complex (TONs 110 and 230, respectively), authors accounted it to a steric factor. The **RuPt-6** complex provides TON 130 and is equally efficient as the **RuPt-7** complex. Thus, the approach using π-extended bridging ligands seems to be reasonable and perspective.
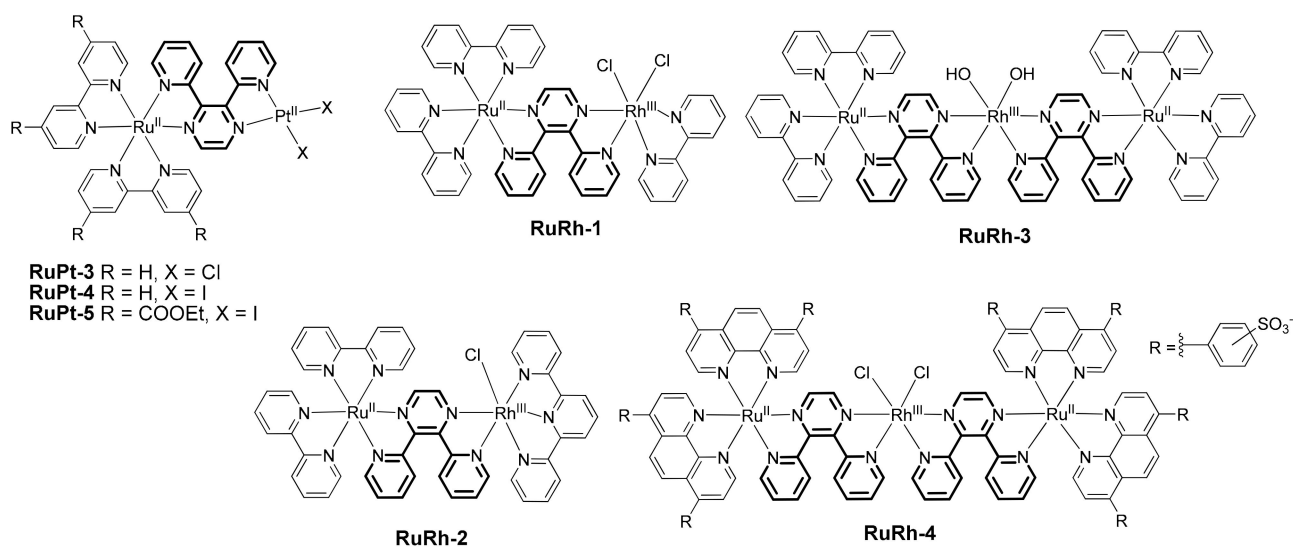
Figure 3. Heteropolynuclear 2,3-bis(pyridin-2-yl)pyrazine complexes for hydrogen photogeration.
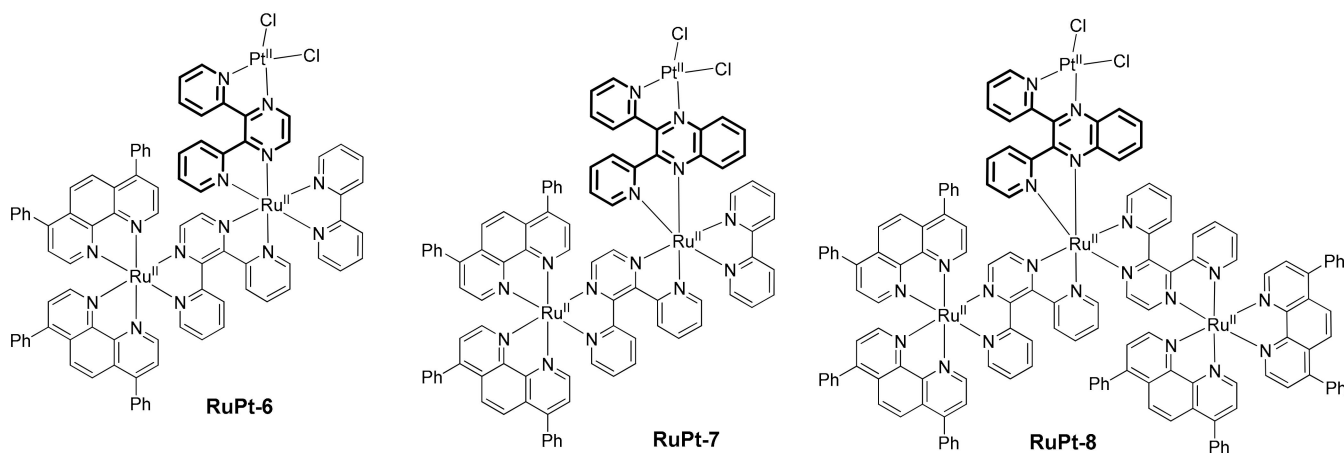

Figure 4. Heteronuclear Ru-Pt complexes with 2,3-bis(pyridin-2-yl)pyrazine and 2,3-bis(pyridin-2-yl)quinoxaline.

There are many examples of supramolecular photocatalysts in which bridging ligands possess azine moieties organized in one heteroaromatic system. A classical ligand of this type is tetrapyridophenazine and its derivatives. Rau et al. [47–49], in order to optimize the catalytic center and peripheral ligands, studied **RuPd-5**, **RuPt-9** and **RuPt-10** complexes (Figure 5). These catalysts provided the following TONs in the photogeneration of hydrogen: 238 (18 h), 7 (18 h), and 279 (70 h), respectively. The **RuPt-10** complex is notable for its high stability under reaction conditions, which helped to increase the reaction time up to 70 h and also to increase TON. Mengele and Raw [50] were the first to propose a promising **RuRh-5** complex, which is also characterized by increased stability. Palladacycle-containing **RuPd-6** complex was studied in [51]. A comparison of **RuPd-5** and **RuPd-6** complexes revealed that the latter is less efficient but retains activity better over long time spans (25 h). The authors also studied the formation of colloidal Pt and Pd in the course of the reaction and found out that Pt complexes are much less prone to this process. The **RuPt-11** NHC complex was studied in [52], and it demonstrated higher activity than the **RuPt-9** complex; moreover, the efficiency of **RuPt-11** can be increased in the presence of iodides due to in situ ligand exchange.
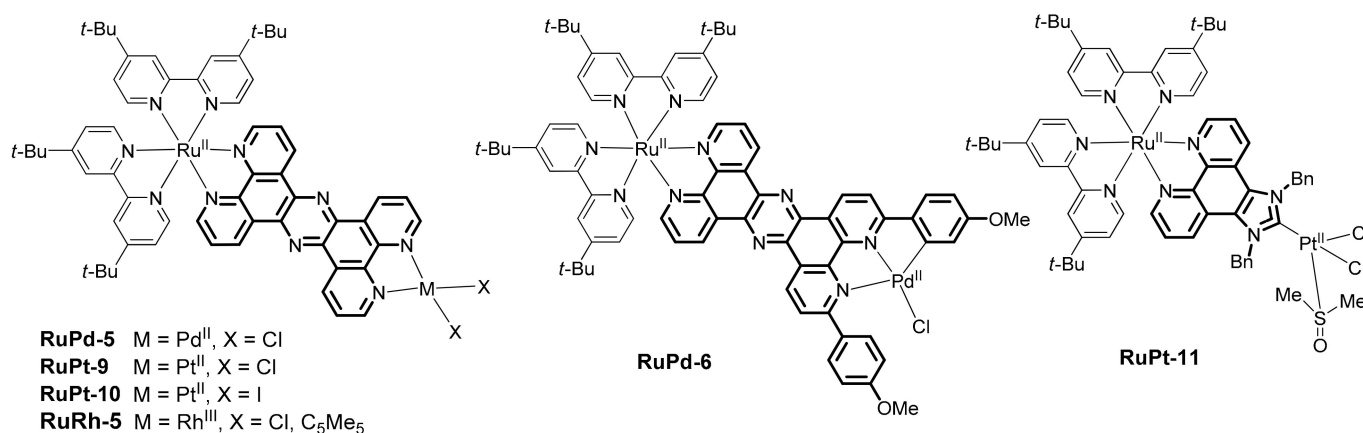
Figure 5. Examples catalysts based on tetrapyridophenazine and imidazophenanthroline.

Another studied type of supramolecular photocatalysts consists of systems without π-conjugation between azine ligands. The Pd and Pt binuclear complexes **RuPd-7**, **RuPd-8**, **RuPt-12** and **RuPt-13** (Figure 6) were studied in [53]; these complexes contain 2,2′:5′,3″:6″,2‴-quaterpyridine as a bridging ligand. **RuPd-8** with electron-withdrawing substituents demonstrated the best TON 489 in 18 h, which is higher than for the majority of Pd complexes with other bridging ligands. **RuPt-14** complex featuring bis(1,10-phenanthroline) ligand (Figure 6) was found to be insufficiently robust under the reaction conditions, and the formation of hydrogen was mainly due to the Pt colloid formed during the decomposition of this complex.
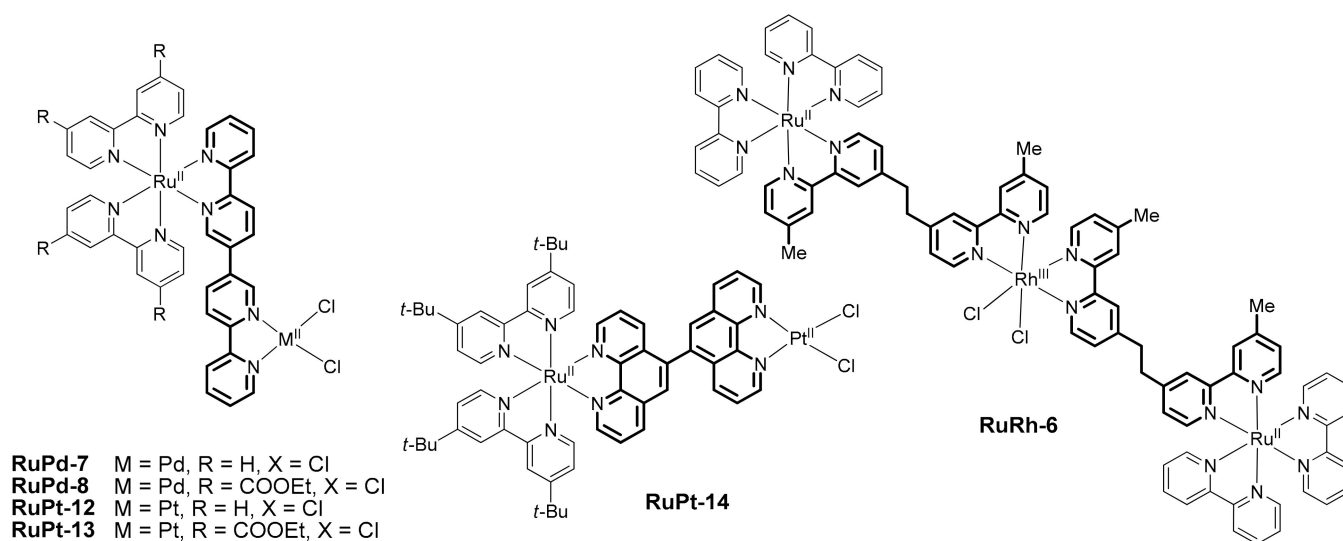

Figure 6. Catalysts based on linked 1,10-phenanthroline and 2,2′-bipyridine.

The trinuclear complex **RuRh-6** (Figure 6) with a flexible linker was studied in [54]. It was shown to be active in hydrogen photogeneration in a water solution and provided good TON. The covalent bonding of the photocatalyst with the Rh(III) complex provides not only a higher TON compared to mixed catalytic systems but also leads to better catalyst stability under the reaction conditions.

The work by Elias et al. [55] was dedicated to a comparison of the supramolecular catalysts **IrCo-1**–**IrCo-6** (Figure 7) and the elucidation of the influence of the ligands' nature in the photoactive Ir(III) complexes on the catalysts' activity. The position of the linker in 2,2′-bipyridine core, providing better interaction of Ir(III) and Co(III) complexes on the catalyst efficacy, was also studied.
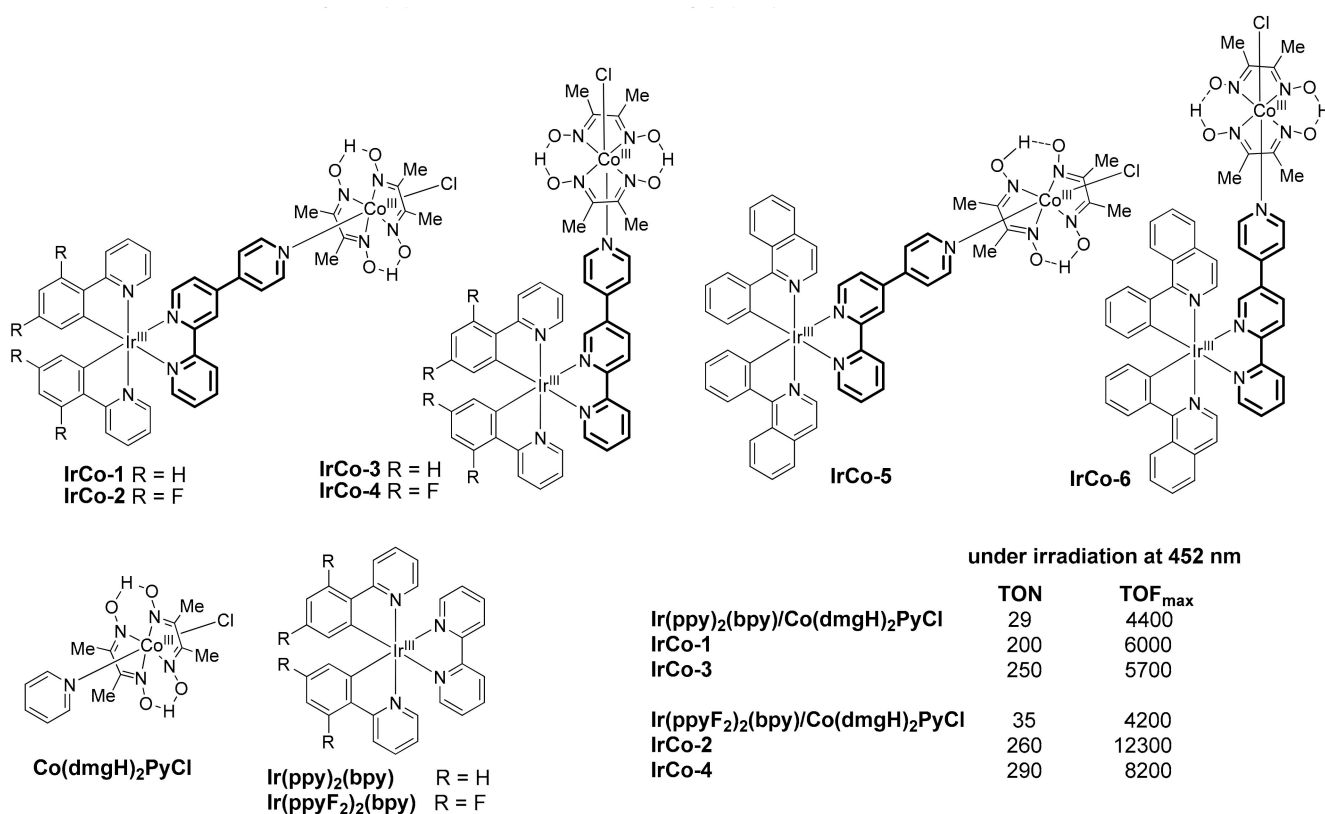
under irradiation at 452 nm

	TON	TOF$_{max}$
Ir(ppy)$_2$(bpy)/Co(dmgH)$_2$PyCl	29	4400
IrCo-1	200	6000
IrCo-3	250	5700
Ir(ppyF$_2$)$_2$(bpy)/Co(dmgH)$_2$PyCl	35	4200
IrCo-2	260	12300
IrCo-4	290	8200

Figure 7. Heterobinuclear Ir-Co complexes based on terpyridine ligands and similar mixed catalytic system.

These complexes can be considered a clear example of the advantage of a supramolecular photocatalyst over a mixed catalytic system. Thus, under the same conditions, supramolecular photocatalysts **IrCo-1**–**IrCo-4** provide 6–11 times higher TON and up to 2 times higher TOF (Figure 7) than the mixture of Co(III) complex and the corresponding photocatalyst. It was found that the catalyst's activity depends on the wavelength of the irradiation. Blue light (452 nm) was efficient for **IrCo-6** and **IrCo-2** complexes, and yellow and red light provided best the TONs for **IrCo-3** and **IrCo-6**, in spite of the fact that the absorbance of light is governed by the nature of the additional ligands and not of the bridging ligand. Authors suppose that the use of π-extended ligands allowed the reaction under irradiation with a red light of lower energy.

Recently, Rau et al., have compared **RuRh-5**, **RuRh-7** and **RuRh-8** complexes (Figure 8), differing by the structure of the bridging ligand. Photocatalytic formate-driven reduction of nicotinamide (3-pyridinecarboxamide, NAD) into NADH (1,4-dihydropyridine-3-carboxamide) was employed as a model reaction. A key step of the process was the two-electron reduction leading to the Rh(I) complex, which is provided by the photoinduced electron transfer from the Ru complex. For each of these supramolecular catalysts, similar TONs were observed when conducting the reaction under thermal conditions without irradiation. Under irradiation, the **RuRh-8** catalyst showed the best activity at 25 °C, as well as at other temperatures, while **RuRh-7** and **RuRh-8** catalysts demonstrated similar TONs and TOFs at 45 °C for 90 min. A series of spectral investigations disclosed that the key feature of an efficient catalytic system is the high rate of the first electron transfer between photoactive and catalytic centers.
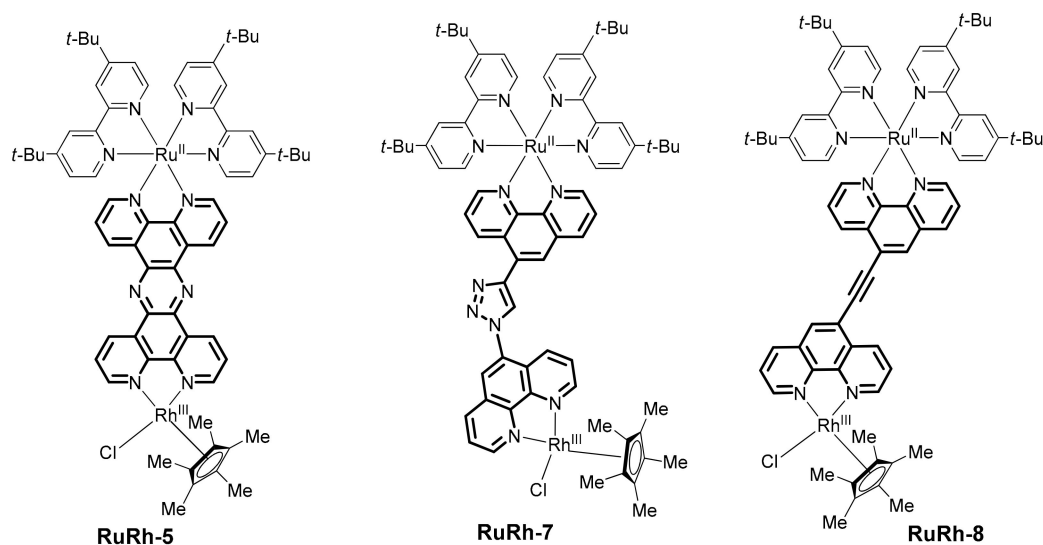
Figure 8. Heteronuclear Ru-Rh complexes based studied in [56].

Thus, the above-mentioned examples clearly demonstrate wide opportunities for catalytic system optimization by selecting the structure of the bridging ligand depending on the chemical nature of the photoactive and catalytic centers, as well as peripheral ligands of these centers.

2.2. Heterobinuclear Complexes for Photocaytalytic CO_2 Reduction

The reduction of CO_2 into CO is a perspective process for diminishing CO_2 content in the atmosphere and further use of carbon monoxide as a C1 synthone in organic transformations. The use of visible light is considered to be an ecologically friendly energy source. The general principle of CO_2 photoreduction using supramolecular photocatalysts is shown in Scheme 3 [20]. The catalyst consists of the photosensitizer (PS) and metal complex catalyst (Cat). Under irradiation, the photosensitizer transforms into an excited state which can donate an electron to the catalyst (oxidative quenching) or accept electrons from the reductant (reductive quenching). The reductive quenching is also followed by the electron transfer to the catalyst. In the first way, the supramolecular catalyst can relax to the ground state via the next electron transfer, so the second way is considered to be preferable.

$$CO_2 + 2e + 2H^+ \longrightarrow HCOOH$$
$$CO_2 + 2e + 2H^+ \longrightarrow CO + H_2O$$
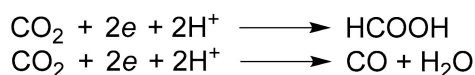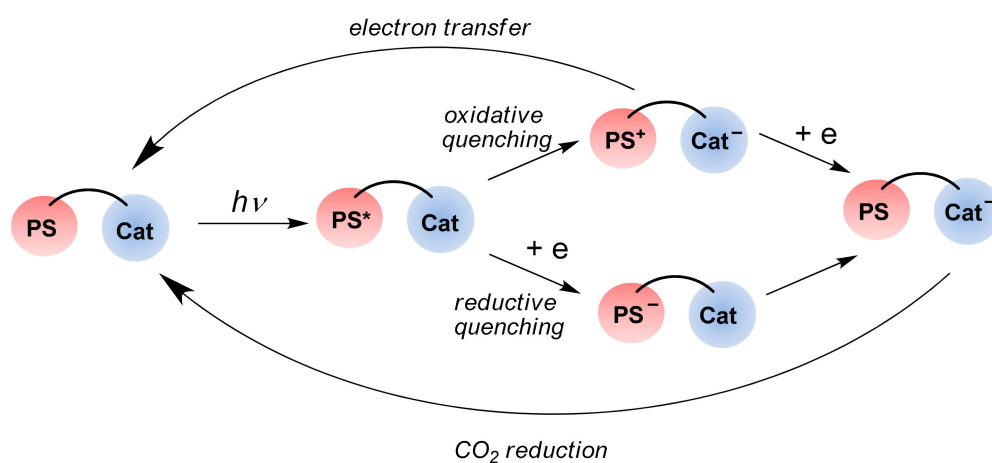
Scheme 3. General mechanisms of CO_2 photoreduction [29]. PS—Photosensitizer, Cat—Catalyst.

In the elaboration of photocatalysts for CO_2 reduction, one needs to ensure the stability of the catalyst and high TONs, and on the other hand, a good selectivity of the catalyst is also demanded in order to prevent the formation of hydrogen, which is a side reaction in this process.

The following compounds are used as sacrificial electron donors in this transformation: sodium ascorbate, 1-benzyl-1,4-dihydronicotinamide (BNAH), 1,3-dimethyl-2-phenyl-2,3-dihydro-1H-benzo[d]imidazole (BIH) and triathanolamine (TEOA). The group of Kimura was the first to propose **RuNi-1**–**RuNi-3** binuclear complexes (Figure 9) on the basis of photoactive Ru(II) complexes and Ni(II)-cyclam complex bound by a flexible linker for CO_2 reduction [57–59]. The authors demonstrated better selectivity of the binuclear catalysts compared to mixed the catalytic system; however, their TONs were low. **RuNi-4**, **RuCo-1** and **RuCo-2** complexes containing bis(1,10-phenanthroline) bridging ligands were synthesized by Komatsuzaki et al. [60], but they also demonstrated low TONs and insufficient CO/H_2 selectivity.
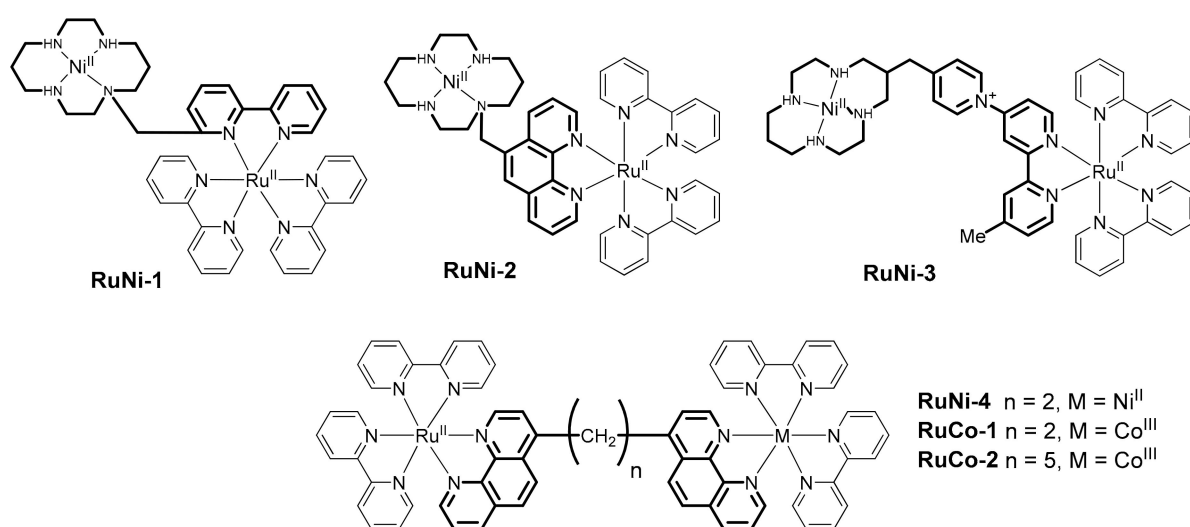

Figure 9. Ru-Ni and Ru-Co heteronuclear photocatalysts.

A veritable progress in the creation of supramolecular photocatalysts for the selective reduction of CO_2 into CO was achieved by Ishitani et al. [29,31]. In 2005, they proposed supramolecular photocatalytic systems containing a Ru(II) photoactive complex and Re(I) complex [61]. Several catalytic systems, **RuRe-1**–**RuRe-5,** were studied, which differ by the linker type, orientation, and the position of substituents in the photoactive complex (Figure 10).

The **RuRe-2** complex with a flexible linker and electron donor substituents was shown to provide the best activity and selectivity in this series, and only this complex outperforms other mixed catalytic systems in TON value. It was also disclosed that the combination of several Re(I) complexes and one Ru(II) complex in one molecule helps to further increase TON.

Successive studies had the goal of revealing optimal combinations of the ligands in the Re(I) complex, substituents in the Ru(II) complex and the structure of bridging ligands. The investigation of **RuRe-6**–**RuRe-8** complexes (Figure 11) showed that an increase in the length of the linker between Re(I) and Ru(II) complexes from C2 (**RuRe-6**) to C4 and C6 led to a decrease in the catalytic activity of the complexes [62]. Bian et al., compared **RuRe-6** and **RuRe-9** complexes and demonstrated that with the same linker length, π-conjugation resulted in a twofold diminishing of TON [63]. Authors assumed that this was due to the lowering of the π* orbital energy of the Re(I) complex, which led to poorer catalytic activity. This fact is consistent with the results obtained earlier for **RuRe-4** and **RuRe-5** complexes which also contain π-conjugated bridging ligands [61]. Thus, in some cases, conjugation can disfavor the electron transfer.
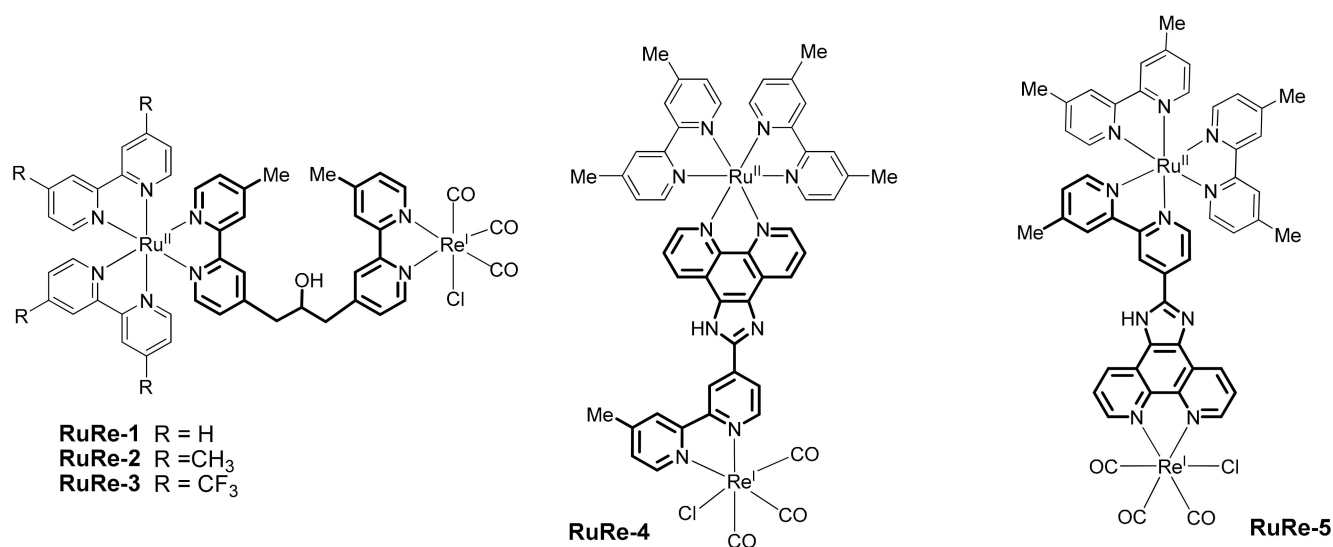
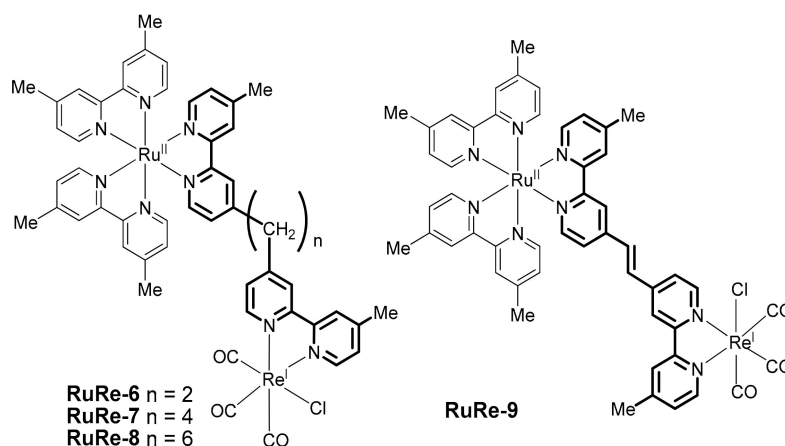**Figure 10.** Ru-Re heteronuclear photocatalysts developed in [61].

Figure 11. Ru-Re heteronuclear photocatalysts with various aliphatic linkers.

The works [64–66] of Ishitani et al., studied in detail the processes of photoinduced electron transfer in **RuRe-10**–**RuRe16** complexes (Figure 12) and their catalytic activity in the CO_2 reduction reaction. The introduction of the electron-withdrawing oxygen in the structure of bridging ligand allows an increase in the catalytic activity of the **RuRe-10** complex compared to **RuRe-12** and **RuRe-13** complexes. On contrary, sulfur-containing bridge led to a low photostability of the complex **RuRe-11**. The analysis of the electron transfer rate revealed its increase in the series **RuRe-15** < **RuRe-14** < **RuRe-10** < **RuRe-13** < **RuRe-16**. However, the highest TON was achieved for **RuRe-10**, while for **RuRe-16** it was two times lower (253 and 123, respectively) [67,68]. It is obvious that the variation of the geometry of the bridging ligand allows for a fine-tuning of the electron interactions of photoactive and catalytic centers.
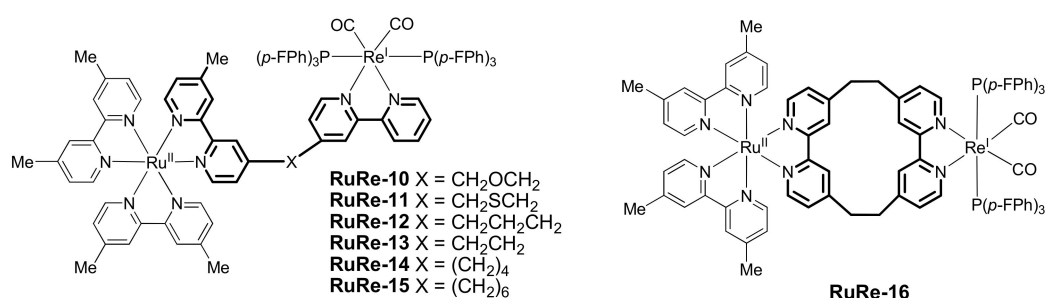
Figure 12. Ru-Re heteronuclear photocatalysts with various flexible linkers.

The catalytic activity of **RuRe-17** and **RuRe-18** (Figure 13) binuclear complexes with a short sulfur-containing linker in CO_2 photoreduction was investigated in [69]. The TONs of these catalysts were humble compared to the above-mentioned complexes; nevertheless, the **RuRe-18** catalyst with an electron-withdrawing SO_2 linker, allowing photoinduced electron transfer from Ru(II) complex, showed superiority over mixed catalytic systems. Both catalysts were found to be unstable (as was **RuRe-11** complex) due to C-S bond cleavage.
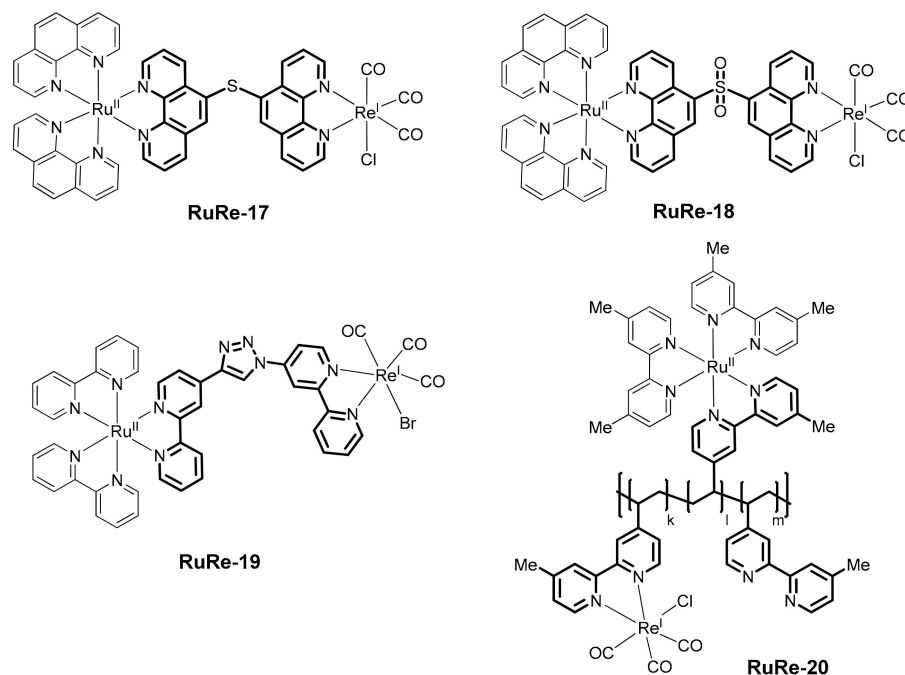

Figure 13. Ru-Re heteronuclear photocatalysts with various linkers.

The binuclear complex **RuRe-19** was synthesized using «chemistry on complex» approach via a classical CuAAC reaction [70]. The authors could not obtain TON better than that of the mixed catalytic system. They supposed that it was due to a delocalization of the first electron, which was produced by a photoexcited Ru(II) complex, at π* orbitals of the bridging ligand. Nevertheless, the two-electron reduction of Re was observed, which is helpful for further the development of such catalysts in other reactions.

Various possibilities of immobilization of binuclear complexes on solid supports are being investigated, both for the creation of photoelectrocatalytic systems and to increase catalysts' efficiency [71,72]. For example, recently, a hybrid polymer **RuRe-20** with tethered Ru(II) and Re(I) complexes has been described [73], which demonstrated different activity in CO_2 reduction into CO depending on the ratio of Re and Ru in the polymer. The most active and best TONs were found for the polymer with an Re:Ru ratio of 1:19.

The advantage of supramolecular **RuRe** photocatalysts over a mixed catalytic system in the CO_2 reduction can be clearly seen by comparing the activity of the **RuRe-21** complex and a mixture of complexes $Ru(4dmb)_3^{2+}$ and *fac*-Re(4dmb)$(CO)_3$Cl (Figure 14). The binuclear complex provides a twofold higher TON, a 2.5-fold higher quantum yield of the reaction, as well as a higher selectivity of CO formation.
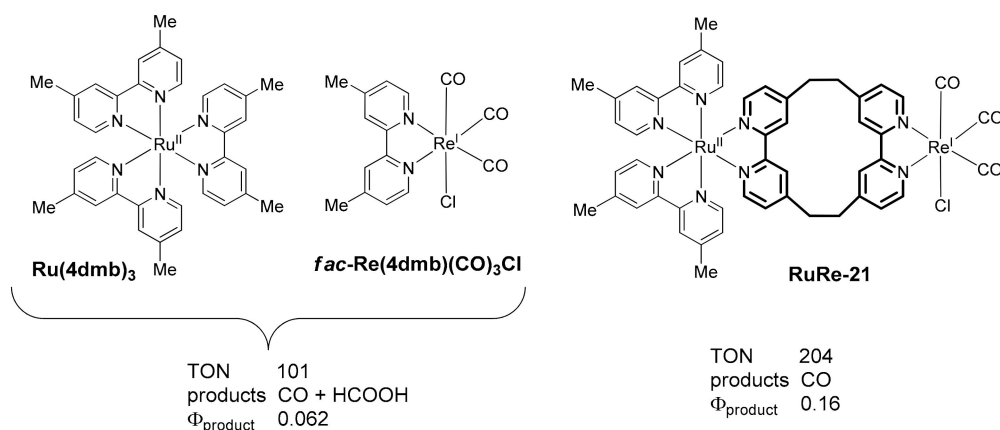

Figure 14. Comparison of the efficiency of the mixed catalytic system ($Ru(4dmb)_3^{2+}$ + *fac*-Re(4dmb)$(CO)_3$Cl) and binuclear catalyst **RuRe21**.

Ishitani et al., described supramolecular photocatalysts **RuMn-1** and **RuMn-2** (Figure 15) in which Re is substituted by a cheaper Mn [74]. The **RuMn-1** complex is more active than **RuMn-2** and the corresponding mixed catalytic system. Unlike with **RuRe** complexes, selectivity of CO_2 reduction is lower, and the main product is HCOOH.
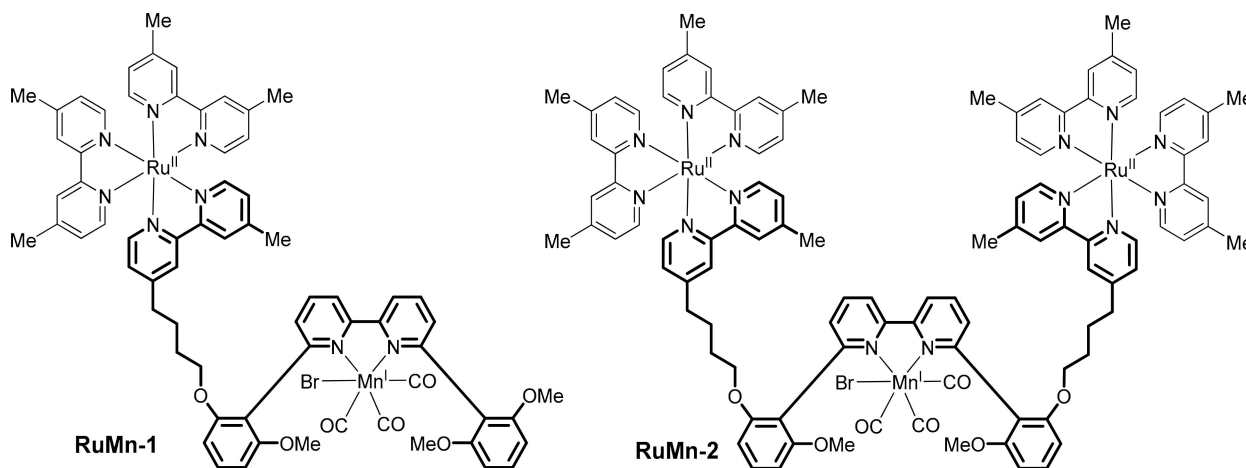

Figure 15. Ru-Mn heteronuclear catalysts for CO_2 reduction.

It is worth noting a significant progress during the last years in the chemistry of Re(I) complexes, covalently linked with the photosensitizers, on the basis of porphyrins [60,75–82]. These compounds demonstrated excellent activity in CO_2 reduction but this chemistry is beyond the frames of the present review.

2.3. Heterobinuclear Photocatalysts in Organic Synthesis

The examples described above demonstrate a great variety of available bridging ligands and complexes on their basis, which opens wide the possibilities of fine-tuning the catalytic systems. The nature and rigidity/flexibility of bridging ligands and the distance between photoactive and catalytic centers provide means to direct the electron and energy transfer. RedOx potential of the photocatalyst can be tuned by the appropriate choice of

the substituents in the additional ligands of Ru or Ir; it also allows optimization of the selectivity and rate of the catalytic process. Application of this experience for creating efficient catalysts for visible light-driven reactions seems to be very promising.

2.3.1. Dimerization of α-Methylstyrene

One of the first reactions of the photocatalytic C-C bond formation using binuclear photocatalysts is a selective radical-free coupling of α-methylstyrene proposed by Inagaki and Akita [83] (Scheme 4).
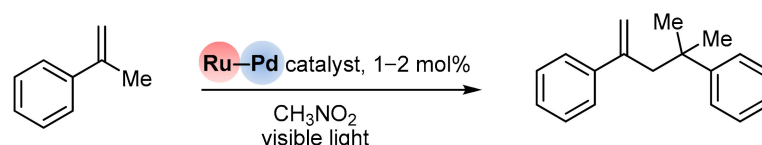
Scheme 4. Photocatalytic dimerization of α-methylstyrene.

Binuclear complexes **RuPd-9**–**RuPd-22** with 2,2-bipyrimidine derivatives as bridging ligands were studied as catalysts in this process (Figure 16).

RuPd-9 R₁ = H; R₂ = H
RuPd-10 R₁ = H; R₂ = Br
RuPd-11 R₁ = Me; R₂ = H
RuPd-12 R₁ = Me; R₂ = Br
RuPd-13 R₁ = tBu; R₂ = H
RuPd-14 R₁ = tBu; R₂ = Br
RuPd-15 R₁ = OMe; R₂ = H
RuPd-16 R₁ = NMe₂; R₂ = H

RuPd-17 R = H
RuPd-18 R = Me

RuPd-19 R₁ = 2-Naphthyl; R₂ = H; R₃ = Br
RuPd-20 R₁ = CH₂CH₂(2-Naphthyl); R₂ = Me; R₃ = Br
RuPd-21 R₁ = 2-Naphthyl; R₂ = 2-Naphthyl; R₃ = Br
RuPd-22 R₁ = H; R₂ = H; R₃ = 2-Naphthyl

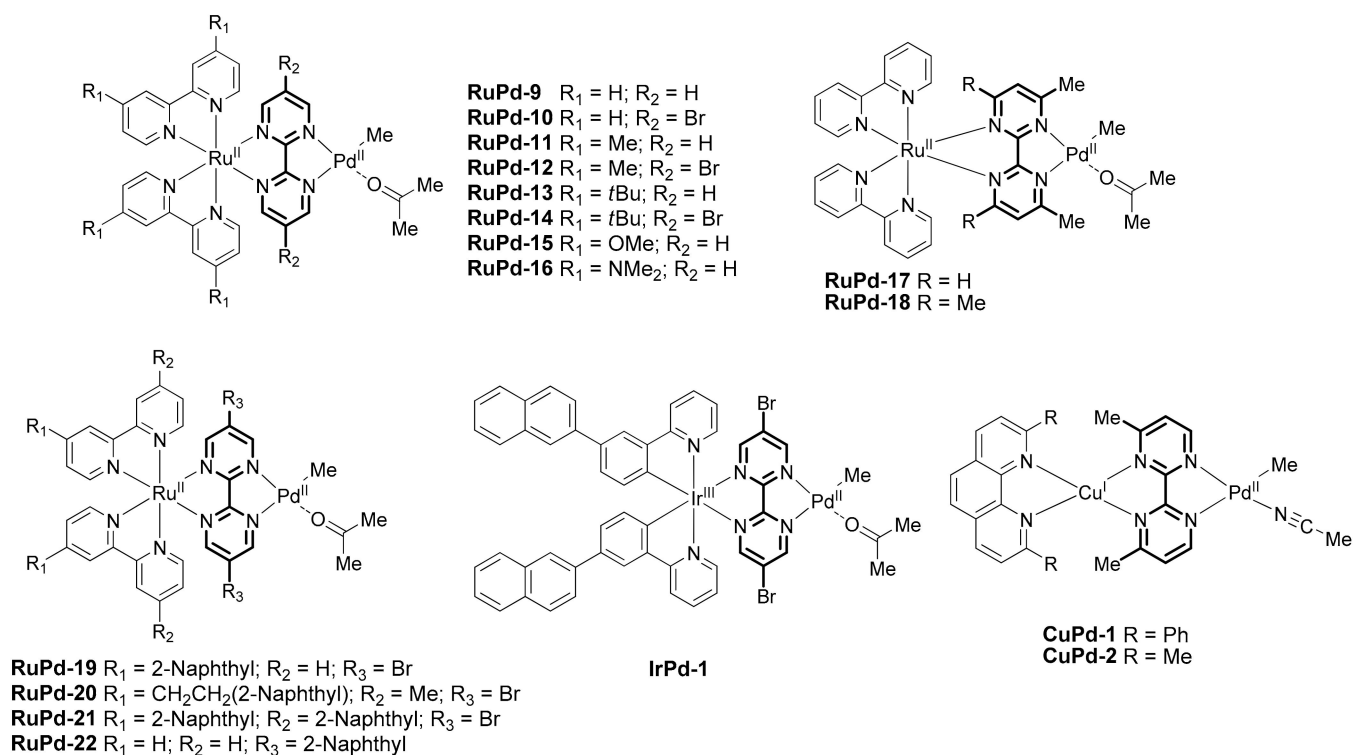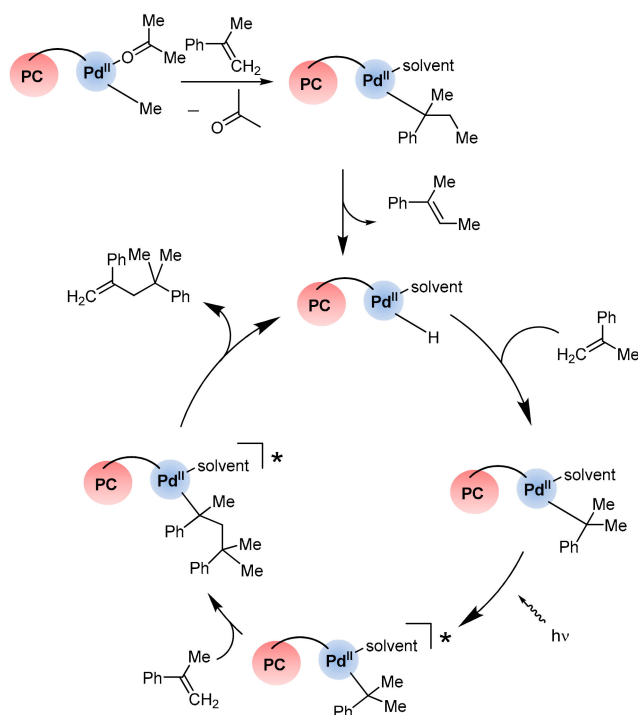**IrPd-1**

CuPd-1 R = Ph
CuPd-2 R = Me

Figure 16. Binuclear photocatalysts for dimerization and polymerization of styrenes.

Authors thoroughly studied the influence of the substituents in the bridging ligand and in 2,2′-bipyridine in the Ru(II) complex on the catalyst selectivity in view of either enhancing the yield of the dimer or promoting polymerization [83–86]. The introduction of electron donor substituents in 2,2′-bipyridine and electron-withdrawing substituents (such as Br) in the bridging ligand led to an increased activity of **RuPd-9**–**RuPd-16** catalysts. The presence of four naphthyl substituents in the photocatalyst increases the lifetime of the excited state of the catalyst and enhances the polymerization rate (**RuPd-20**–**RuPd-22** catalysts), while the **RuPd-19** complex favors the formation of the dimer. The mechanism of the reaction was studied in details using DFT calculations [87] which supported the proposed reaction mechanism (Scheme 5). The Ru(II) complex acts as a light energy harvesting unit, providing the monomer intrusion in the chain and the elimination of

the products from the complex. To note, without irradiation α-methylstyrene does not participate in this reaction.

Scheme 5. Proposed mechanism of photocatalytic dimerization of α-methylstyrene.

The obtained data were used to develop the catalyst for photopolymerization **IrPd-1** (Figure 16) [88]. This catalyst contains the Ir(III) complex as a photoactive moiety. It also provides radical-free polymerization, and it was studied in the copolymerization reaction of styrene with fluorinated vinyl ethers. Under irradiation, styrene participates in the catalytic polymerization while in the darkness polymerization of vinyl ethers takes place. Thus, by switching light on and off the authors succeeded in the controllable copolymerization of styrene with ethers.

Recently, the same group has proposed **CuPd-1** and **CuPd-2** photocatalysts (Figure 16) for polymerization employing the same principle [89]. Cu(I) complexes with 2,9-disubstituted 1,10-phenanthrolines are used as light-harvesting units which are thought to be a cheap alternative to Ru(II) complexes [90].

2.3.2. Other Pd-Catalyzed Reactions

Cross-coupling reactions catalyzed by metal complexes became a versatile and veritable method of organic synthesis for C-C bond formation [91–94]. Complexes and intermediates are transferred into excited state under irradiation, their reaction ability increases and this is employed for catalyzing various processes [12]. However, the reagents are often not able to efficiently absorb visible light which imposes limitations on this approach and demands the application of photosensitizers. In 2007, the photoactivation of Pd-catalyzed Cu-free Sonogashira coupling was demonstrated in the presence of the Ru(bpy)$_3^{2+}$ complex [95]. It was shown later that the covalent binding of (Phen)PdCl$_2$ with BODIPY chromophore results in a higher activity of the catalyst in the copper-free Sonogashira coupling [96].

The activity of **RuPd-23** complex (Figure 17) containing 2,2-bipyrimidine as bridging ligand was studied in the Suzuki-Miyaura reaction [97] (Scheme 6). This binuclear complex showed TON two times higher than a mixed catalytic system (Ru(bpy)$_2$(bpm)$^{2+}$/Pd(bpy)Cl$_2$) under visible light (Table 1, entries 1–4). In the absence of irradiation, no difference in activity was noted. In spite of low TON and humble product yields, the authors demon-

strated the principal superiority of binuclear photocatalyst over the mixed catalytic system. The covalently linked photosensitizer is assumed to generate the Pd(0) complex which participates in the catalytic cycle.
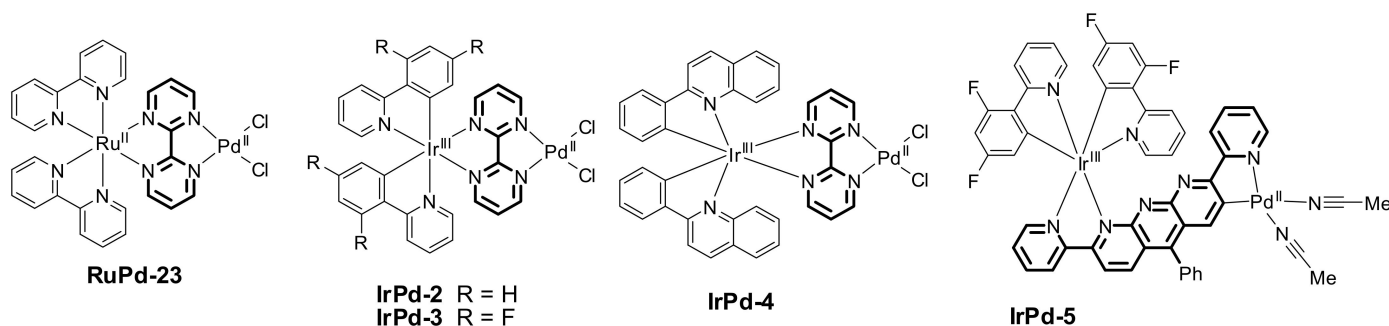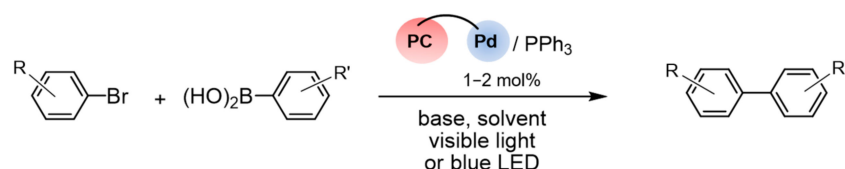

Figure 17. Binuclear photocatalysts for Suzuki-Miyaura and Sonogashira coupling.

Scheme 6. Photocatalytic Suzuki-Miyaura coupling.

Iridium-containing binuclear complexes **IrPd-2**–**IrPd-4** (Figure 17) also were studied in the Suzuki–Miyaura reaction (Table 1, entries 6–8) [98], these complexes also comprise 2,2′-bipyrimidine as a bridging ligand. After optimizing the reaction conditions, the authors established that the best yields in the reaction were provided by the **IrPd-4** complex with π-extended ligands. The authors also studied **RuPd-23** catalyst under adjusted conditions and proved its ability to provide good yields comparable with those obtained with Ir complexes (Table 1, entry 5). The catalyst activity decreases twofold in the darkness (Table 1, entry 9), which supports the photocatalytic character of the reaction. The addition of the phosphine ligand improves the result probably by stabilizing the catalytically active Pd(0) complex. The authors also showed the lower yield of the mixed catalytic system (Table 1, entry 10).

The complex **IrPd-4** was studied using 12 different substrates and provided good to high yields of the products (78–93%).

The authors did not study the reaction mechanism and catalytically active species in detail. The proposed mechanism is given in Scheme 7. It is assumed that the energy transfer from the excited iridium complex to palladium results in its reduction into Pd(0) which participates in the catalytic cycles. The catalyst in an excited state promotes oxidative addition and reductive elimination resulting in the activity enhancement under irradiation with visible light.

Binuclear complex **IrPd-5** (Figure 17) contains iridium and palladacycle [99]. This catalyst was studied with a wide range of substrates (Table 1, Entries 11–15), the authors showed a decrease in the products yields by several times in the darkness as well as in the case of using mixed catalytic system (analogues of the photocatalyst and Pd complex). This catalyst was also studied in the Cu-free Sonogashira coupling (Scheme 8). Under optimized conditions, high yields of the products were obtained using a representative scope of substrates.

**Table 1.** Photoaccelerated energy transfer catalysis of Suzuki–Miyaura coupling with binuclear complexes.

Entry	R	R′	Conditions	Yield, %	Reference
1	H	H	**RuPd-23**/PPh$_3$, (1/2 mol.%) K$_2$CO$_3$, EtOH, r.t., visible light	10	[97]
2	H	H	**RuPd-23**/PPh$_3$, (1/2 mol.%) K$_2$CO$_3$, EtOH, r.t., dark	6	[97]
3	H	H	Ru(bpy)$_2$(bpm)$^{2+}$/ Pd(bpy)Cl$_2$/PPh$_3$ (1/1/2 mol.%) K$_2$CO$_3$, EtOH, r.t., visible light	6	[97]
4	H	H	Pd(bpy)Cl$_2$/PPh$_3$ (1/2 mol.%) K$_2$CO$_3$, EtOH, r.t., visible light	5	[97]
5	Me	H	**RuPd-23**/PPh$_3$, (2.5/5 mol.%) Cs$_2$CO$_3$, DCM-EtOH, r.t., blue LED	80	[98]
6	Me	H	**IrPd-2**/PPh$_3$, (2.5/5 mol.%) Cs$_2$CO$_3$, DCM-EtOH, r.t., blue LED	86	[98]
7	Me	H	**IrPd-3**/PPh$_3$, (2.5/5 mol.%) Cs$_2$CO$_3$, DCM-EtOH, r.t., blue LED	54	[98]
8	Me	H	**IrPd-4**/PPh$_3$, (2.5/5 mol.%)) Cs$_2$CO$_3$, DCM-EtOH, r.t., blue LED	93	[98]
9	Me	H	**IrPd-4**/PPh$_3$, (2.5/5 mol.%)) Cs$_2$CO$_3$, DCM-EtOH, r.t., dark	40	[98]
10	Me	H	Ir(pq)$_2$(bpy)$^+$/Pd(bpm)Cl$_2$/ PPh$_3$ (2.5/2.5/5 mol.%) Cs$_2$CO$_3$, DCM-EtOH, r.t., blue LED	75	[98]
11	MeC(O)	Me	**IrPd-5**/PPh$_3$, (1/2 mol.%) Cs$_2$CO$_3$, MeOH, 30 °C, blue LED	99	[99]
12	MeC(O)	Me	Ir(ppy)$_2$L/[Pd(ppy)Cl]$_2$/PPh$_3$ (1/1/2 mol.%) Cs$_2$CO$_3$, MeOH, 30 °C, blue LED	35	[99]
13	Me	Me	**IrPd-5**/PPh$_3$, (1/2 mol.%) Cs$_2$CO$_3$, MeOH, 30 °C, blue LED	98	[99]
14	CN	Me	**IrPd-5**/PPh$_3$, (1/2 mol.%) Cs$_2$CO$_3$, MeOH, 30 °C, blue LED	98	[99]
15	OMe	Me	**IrPd-5**/PPh$_3$, (1/2 mol.%) Cs$_2$CO$_3$, MeOH, 30 °C, blue LED	78	[99]

Without irradiation, the reaction was shown not to proceed. It is to be noted that the use of the mixed catalytic system Ir(ppy)$_2$L/[Pd(ppy)Cl]$_2$/PPh$_3$ led to a quantitative reduction of ArBr into ArH under visible light. Thus, binding the photoactive component and the catalytic center in one complex gives possibility not only of increasing the catalyst activity but also of improving the reaction selectivity, changing its direction.
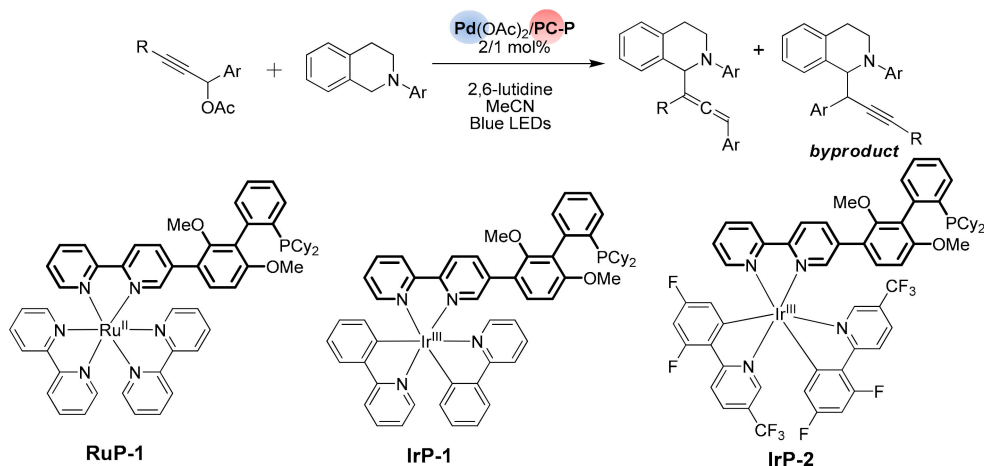
A recent work [100] describes metallaphotoredox catalyzed CH-allenylation of *N*-aryl tetrahydroisoquinolines in the presence of **RuP-1**/Pd(Oac)$_2$, **IrP-1**/Pd(Oac)$_2$ and **IrP-2**/Pd(Oac)$_2$ catalytic systems (Scheme 9).
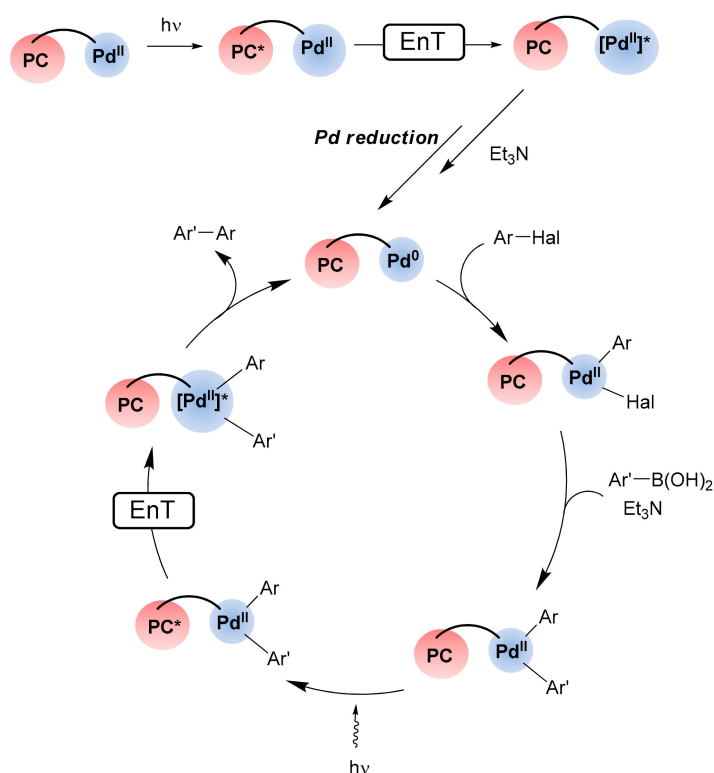
Scheme 7. Proposed mechanism of photocatalytic Suzuki-Miyaura coupling.

$R_1 = CF_3$, $R_2 = H$, 90%
$R_1 = CN$, $R_2 = H$, 95%
$R_1 = Ac$, $R_2 = H$, 97%
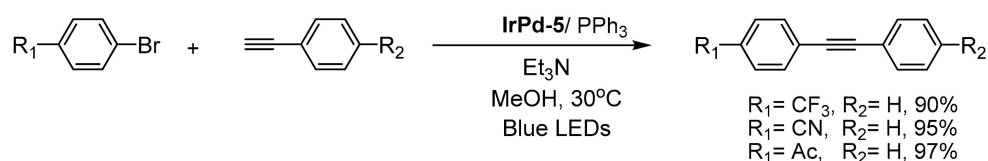
Scheme 8. Photocatalytic Sonogashira coupling.

**Scheme 9.** Photocatalyst-directed Pd-catalyzed allenylation of *N*-aryl tetrahydroisoquinolines.

In this reaction Ru(II) or Ir(III) photoactive complex acts not as a photosensitizer like in the cross-coupling reactions but rather is employed in the generation of the radical from tetrahydroisoquinoline via single electron transfer (Scheme 10), thus, serving as a photoredox catalyst. This radical is trapped in the coordination sphere of palladium followed by the elimination of the acetate anion. After the second intramolecular single electron transfer from photocatalyst to palladium reductive elimination takes place affording the target product.
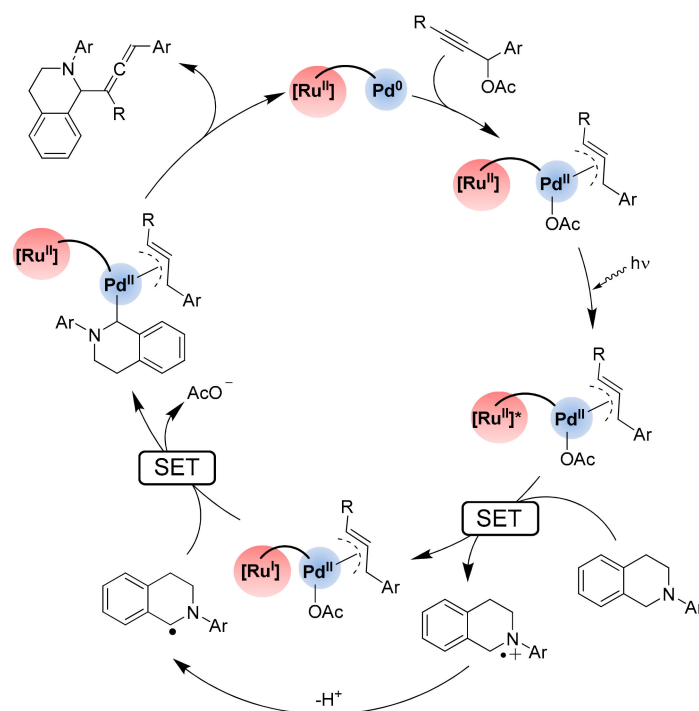
Scheme 10. Proposed mechanism of photoredox-catalyzed allenylation.

The authors studied in situ formed binuclear complexes, starting from **RuP-1**, **IrP-1** and **IrP-2** complexes as a result of Pd coordination to phosphine unit. In this case, bridging ligand is composed of the derivative of Sphos (dicyclohexyl (2′,6′-dimethoxybiphenyl-2-yl)phosphine) ligand with 2,2′-bipyridine moiety, which participates in the formation of the photoactive complex.

The authors demonstrated that mixed catalytic systems with Ru(bpy)$_3$$^{2+}$, as well as with [Ir(ppy)$_2$(dtbbpy)]$^+$, afforded the target product as low as 38% yield and byproduct 40% yield (Scheme 11). Among binuclear catalytic systems, the best conversion and selectivity was shown by the **RuP-1**/[Pd] catalyst (71% yield of target product), while **IrP-1**/[Pd] was somewhat less efficient and **IrP-2**/[Pd] was the least active and selective in this reaction. The authors demonstrated a wide scope of the reaction, target compounds were obtained in 39–73% yields. Thus, the combination of the photoactive complex and metal catalyst increases not only the activity but also the selectivity of the catalytic system.

	Conversion	Yield A	Yield B
Ru(bpy)$_3$/SPhos Pd(OAc)$_2$	78%	38%	40%
RuP-1/Pd(OAc)$_2$	100%	71%	<5%
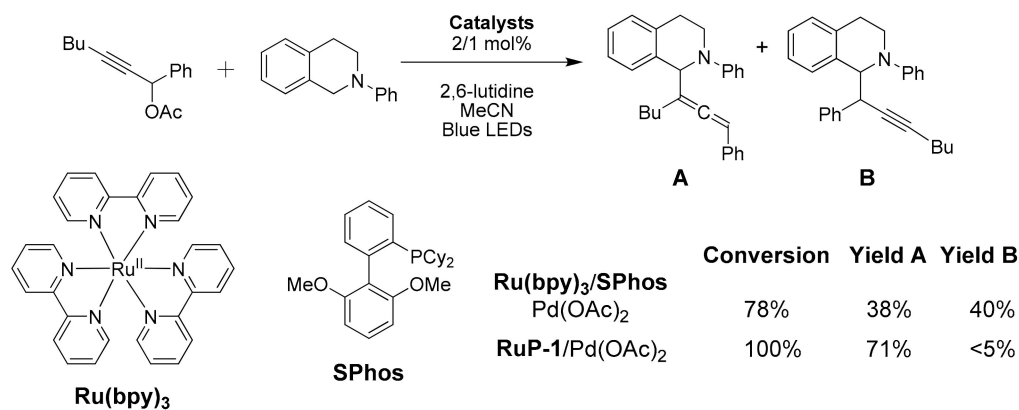
Scheme 11. Comparison of the mixed catalytic system and supramolecular catalyst in photoredox-catalyzed allenylation.

2.3.3. Oxidation Reactions

One of the important directions of photoredox catalysis development under visible light is the elaboration of the catalytic systems capable of selective oxidation of organic substrates under mild conditions at low catalyst loadings. Binuclear photoactive complexes have been extensively studied as photocatalysts for water splitting with oxygen production (so called artificial photosynthesis) [101–103]. The catalytic cycle of such oxidation processes is given in Scheme 12. Photoactive moiety of the complex in an excited state transmits an electron to an outer oxidant (or to anode) followed by intramolecular single electron transfer which leads to the oxidation of the metal complex catalytic center. Two such transfers produce an M=O oxo complex which can either release molecular oxygen or oxidize organic substrates.
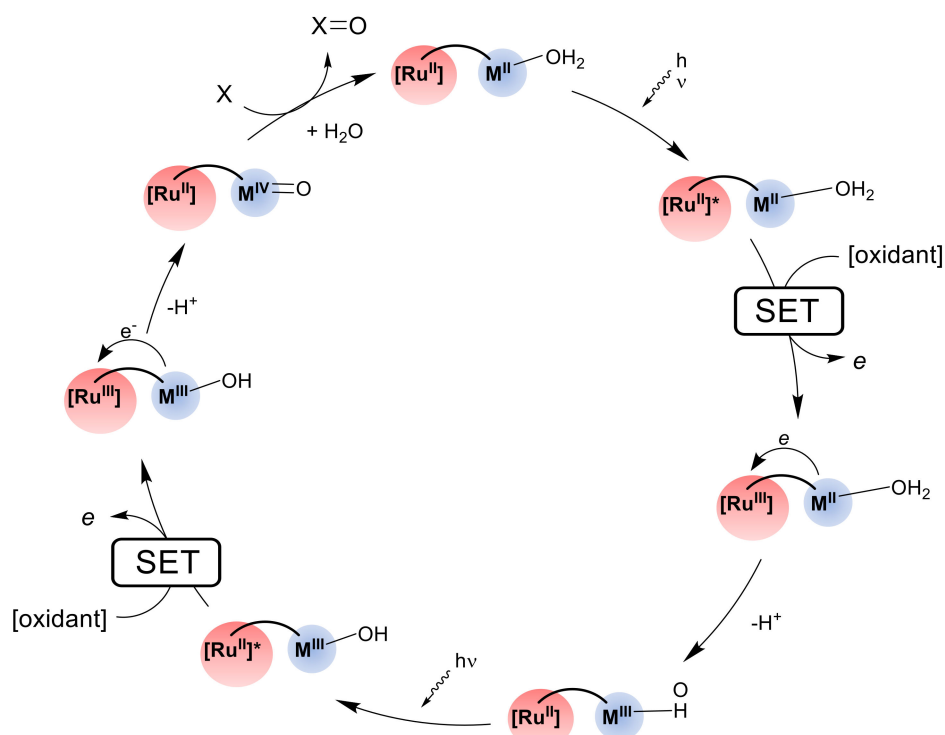
Scheme 12. Mechanism of photocatalysed two-electron oxidation.

Polynuclear complex **Ru₂Ru** was studied as a photocatalyst for selective oxidation of benzylic alcohols into ketones [104] (Scheme 13). Co(III) salt is used as oxidant.

Scheme 13. Photocatalysed alcohol oxidation.

A photoactive moiety of **Ru₂Ru** catalyst contains two Ru(tpy)₂ complexes, and metal catalytic center features Ru(tpy)(bpy) complex (tpy = 2,2′,6′,2″-terpyridine) with a coordinated water molecule (Figure 18). The authors could not achieve high yields of ketones although selectivity of oxidation was remarkable.
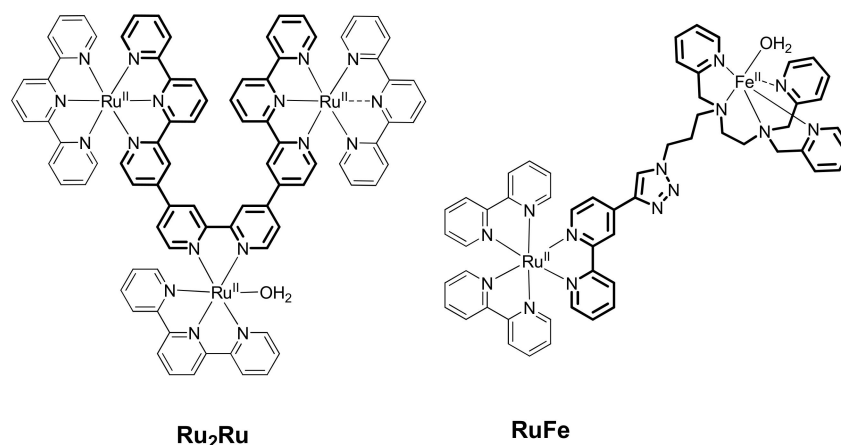
Figure 18. Ru-Ru and Ru-Fe photocatalysts for oxidation reactions.

The binuclear complex **RuFe** with a flexible linker was described in [105]. Its photophysical characteristics were thoroughly studied and the formation of Fe(IV) oxocomplex was established, which can oxidize triphenylhposphine to phosphinoxide. The authors did not study the catalytic properties of this complex, but underline its good potential as a catalyst of oxidation processes.

An important reaction used in organic synthesis is selective oxidation of organic sulfides into corresponding sulfoxides. Due to mild reaction conditions and its high selectivity, photoredox catalysis seems to be the perspective for this process. The oxidation of sulfides into sulfoxides was described for a variety of homogeneous and heterogeneous photocatalysts [106]. Several mechanisms of this process were proposed [107,108], one of them assuming the generation of a singlet oxygen as a result of energy transfer from the photocatalyst in excited state to the molecule of oxygen. The second mechanism includes single electron transfer from the organic sulfide to photocatalyst. In the presence of copper complexes, the oxygen molecule is activated via coordination with Cu(I) which favors the oxidation of the organic substrate.

The binuclear complex **RuCu-1** (Figure 19), in which photoactive Ru(II) complex is bound with Cu(I) complex via a flexible linker, was synthesized and studied in [109]. The authors supposed that this complex can catalyze the oxidation of organic sulfides into sulfoxides according to different mechanisms (Scheme 14), but the key step is inevitably the participation of dioxygen copper complex in the oxidation. The formation of such complexes needs the presence of the Cu(I) complex, which is generated in a series of SET between the Cu(II) complex and the photocatalyst using an external reducing agent.
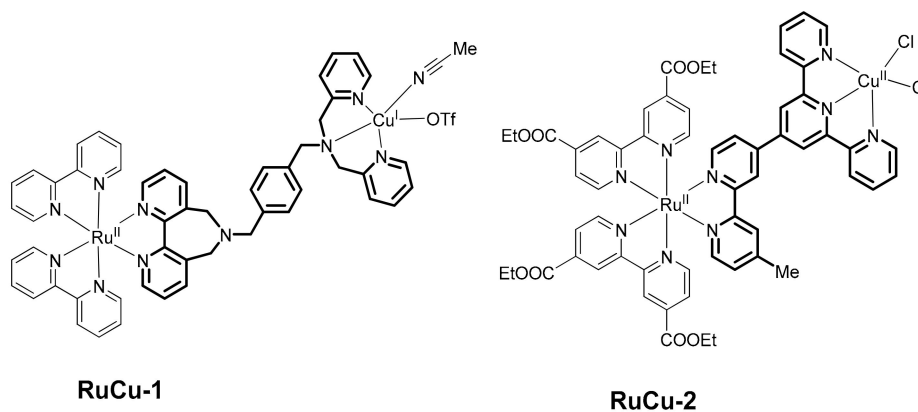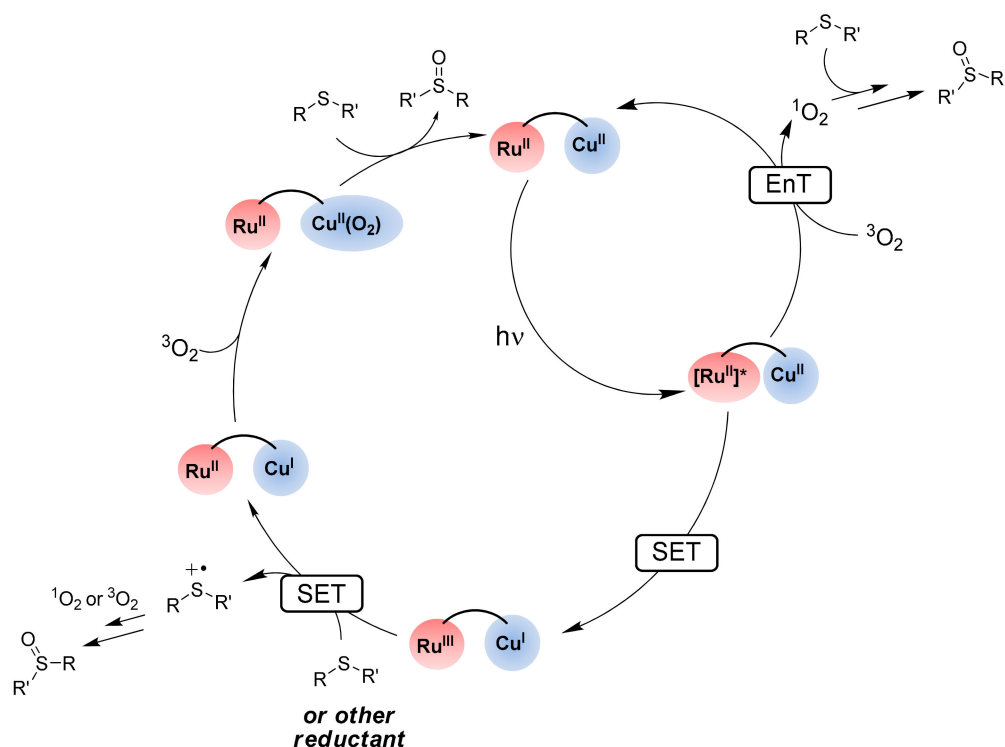

Figure 19. Binuclear photocatalysts for organic sulfides oxidation.

Scheme 14. Mechanisms of organic sulfides oxidation photocatalyzed with binuclear complexes.

The proposed catalytic system (**RuCu-1**) is characterized by high activity and selectivity in the oxidation of sulfides and triphenylphosphine (Scheme 15). Triethanolamine (TEOA) is used as an external reductant. Without photocatalyst, the copper complex was shown to be catalytically inactive and the activity of a mixed catalytic system is 4 times lower. Moreover, the results are essentially the same as those obtained with $Ru(bpy)_3^{2+}$ without the copper complex. Thus, it is the covalent binding of the photoactive and metal complexes which provides high catalytic activity. The authors reached TON 300 at 60% conversion with 100% selectivity.
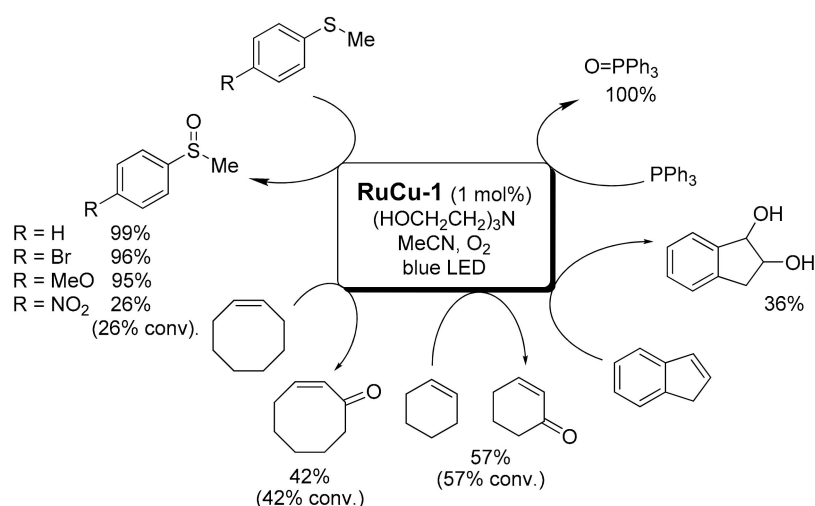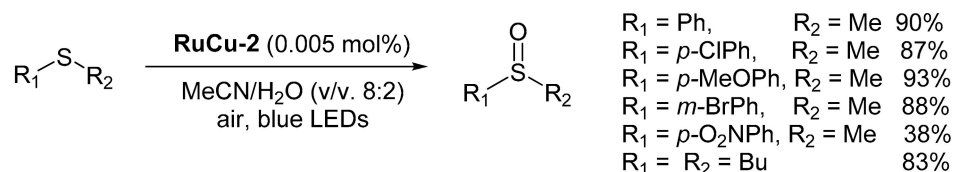

Scheme 15. RuCu-1 in photocatalyzed oxidation reactions.

Aerobic oxidation of indene in the presence of **RuCu-1** under analogous conditions led to a corresponding *cis*-diol in 37% yield with 100% conversion of starting indene. Oxidation of cyclohexene and *cis*-cyclooctene gave desirable α,β-unsaturated ketones in 57 and 42%

yields, respectively, with 100% selectivity (Scheme 15). The authors propose this catalytic system as a promising alternative to classical oxidants.

Complex **RuCu-2** (Figure 19) with a more rigid bridging ligand and electron-withdrawing substituents in the photoactive Ru(II) complex was described in [110] for the aerobic oxidation of organic sulfides. The majority of substrates provided high yields of the oxidation products (Scheme 16) in the presence of as low as 0.005 mol.% catalysts, which is equivalent to TON ca. 18,000, while in a special experiment TON was increased to an incredibly high 32,000. Despite the fact that the reaction time is significantly increased due to the low loading of the catalyst, it demonstrates a high stability of the catalyst under the reaction conditions.

$R_1 = Ph,$ $R_2 = Me$ 90%
$R_1 = p\text{-ClPh},$ $R_2 = Me$ 87%
$R_1 = p\text{-MeOPh},$ $R_2 = Me$ 93%
$R_1 = m\text{-BrPh},$ $R_2 = Me$ 88%
$R_1 = p\text{-O}_2\text{NPh},$ $R_2 = Me$ 38%
$R_1 = R_2 = Bu$ 83%

Scheme 16. Oxidation of organic sulfides to sulfoxides with **RuCu-2** catalyst.

2.3.4. Catalysis by Ni, Mn and Au Containing Complexes

One of the most important achievements in merging photoredox and transition metal catalysis is the possibility of employing cheaper catalysts on the basis of Ni complexes in various reactions of carbon–carbon and carbon–element bonds formation [11,111]. Among other reactions, it is the case of cross-coupling reactions of aryl halides with various nucleophiles. Single electron transfers between nickel complexes and photocatalysts allow to generate in the frames of one catalytic cycle both Ni(0), assuring oxidative addition, and Ni(III), providing efficient reductive elimination (Scheme 17). It would be quite expectable that the combination of Ni complex and photoredox active component in one compound increases the activity of the catalytic system.
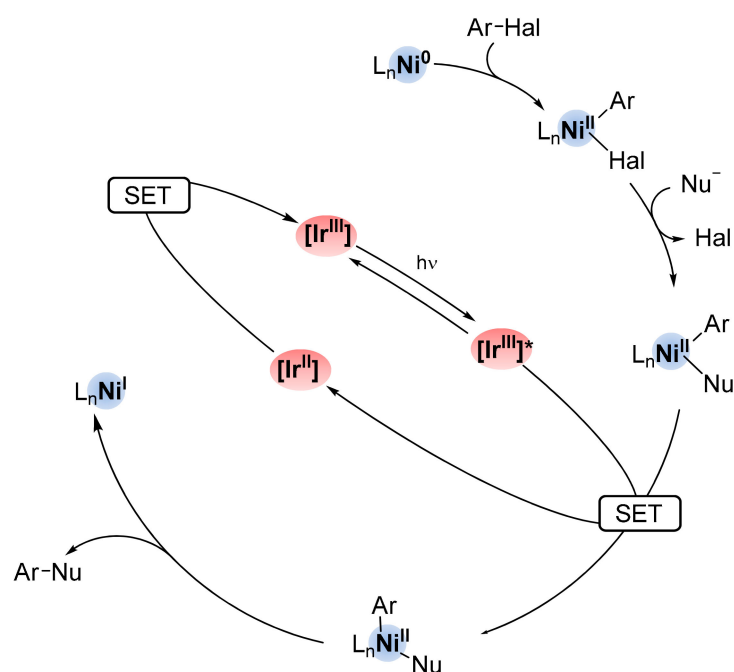
Scheme 17. Proposed mechanism of Ni-photocatalyzed carbon–heteroatom coupling.

In a recent work [112], a series of binuclear Ir-Ni complexes with different bridging ligands has been studied in the catalytic coupling of aryl and vinyl bromides (Scheme 18) with carboxylic acids. Binuclear complexes were generated in situ from **IrN-1–IrN-5** complexes (Figure 20) and Ni(II) complex.
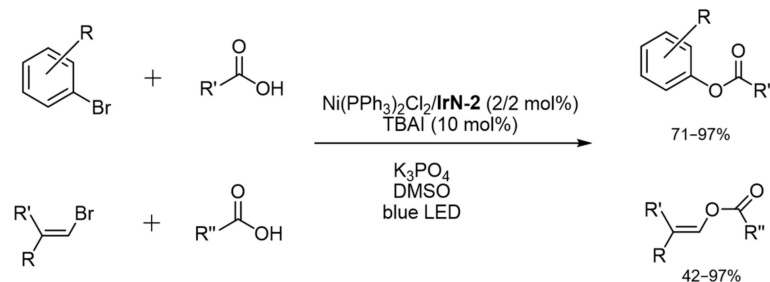
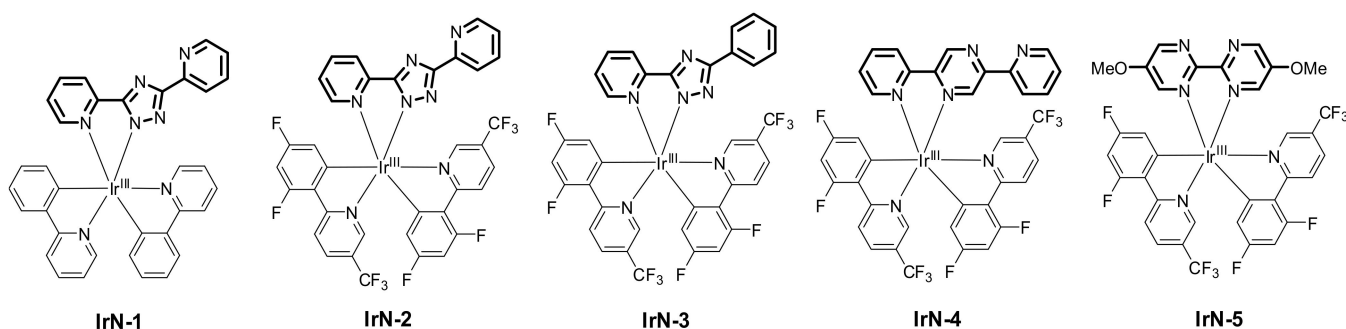**Scheme 18.** Cooperative Ir-Ni-photocatalysis for coupling of aryl- and vinyl bromides with carboxylic acids.

Figure 20. Ir-complexes for generation Ir-Ni-complexes in situ.

The authors have found that only the **IrN-2**/Ni(PPh$_3$)$_2$Cl$_2$ catalytic system provides high yields of the coupling products with aryl and vinyl bromides (Scheme 18). It is important that the target compound can be obtained only with **IrN-1**/Ni(PPh$_3$)$_2$Cl$_2$ or **IrN-2**/Ni(PPh$_3$)$_2$Cl$_2$ systems, other complexes as well as mixture of complexes were inactive under the same reaction conditions. Thus, the presence of bridging ligand in the compound and its nature are important for the reaction to occur.

The same catalytic system was shown to be applicable to Ni-catalyzed reactions of C-S and C-N coupling (Scheme 19).
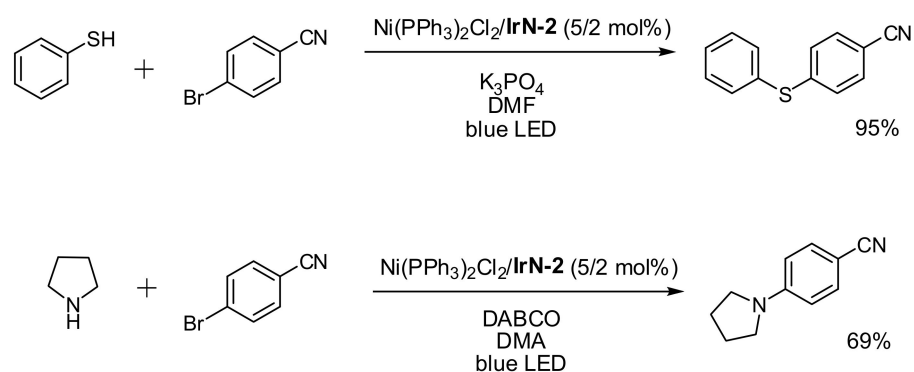
Scheme 19. C-S and C-N coupling catalyzed with Ir-Ni binuclear complex.

The binuclear complex **RuMn-3** with 2,2′-bipyrimidine as a bridging ligand [113] was employed as a co-catalyst of the copper-catalyzed azide-alkyne [3+2] cycloaddition (Scheme 20).
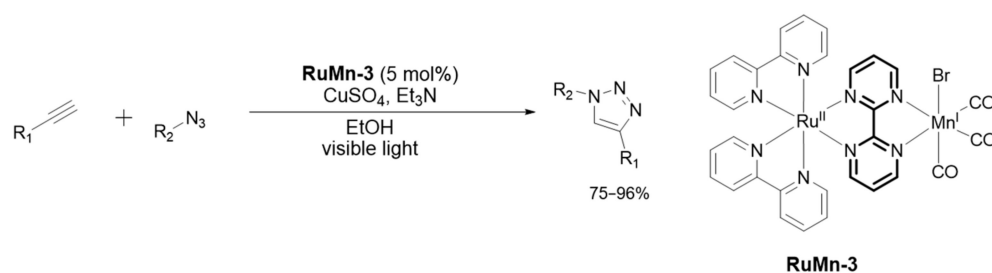
Scheme 20. Visible light-assisted copper-catalyzed azide-alkyne [3+2] cycloaddition.

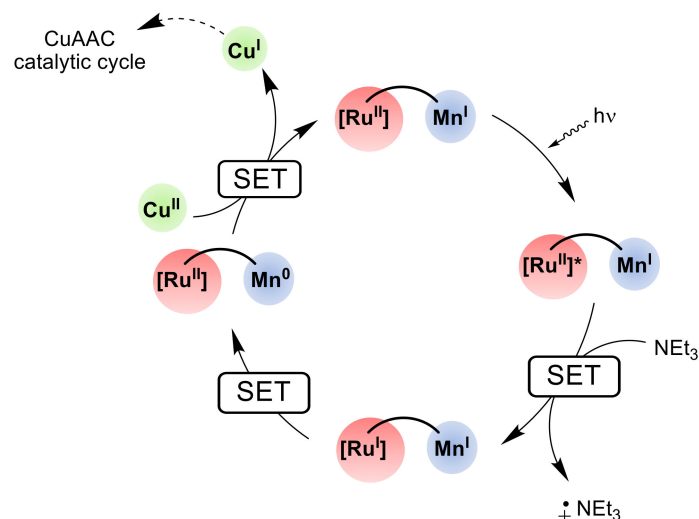The photoactive complex does not participate directly in the catalysis of this process but rather acts as a photoredox catalyst (Scheme 21). Under irradiation with visible light, the binuclear complex provides the reduction of Cu(II) into Cu(I) with triethylamine via several intra- and intermolecular single electron transfers, and Cu(I) catalyzes the reaction.

Scheme 21. Proposed mechanism of visible-light-assisted CuAAC.

The reaction did not proceed without photocatalyst under described conditions. Moreover, the use of only the Mn complex or application of only the photocatalyst were inefficient, and mixed catalytic system $Ru(bpy)_3^{2+}/Mn(bpm)(CO)_3Br$ provided only 46% yield in a model reaction (versus 96% in the case of **RuMn-3**). Thus, only binuclear complex provides required RedOx potential of the catalyst.

A novel catalytic system for the arylation of diethylphosphite with diazonium salts (Scheme 22) has been put forward recently in [114]. Isomeric binuclear complexes **RuAu-1** and **RuAu-2** were used as catalysts which were obtained according to different approaches (sequential complexation for **RuAu-2** and "chemistry on complex" in the case of **RuAu-1**). Both complexes demonstrated similar catalytic activity.

The reaction proceeds according to a radical mechanism with the formation of aryl radical as a result of SET reduction of the diazonium salt (Scheme 23). Authors studied the influence of irradiation, nature of catalyst, and the covalent binding of Ru and Au complexes on the reaction yield.
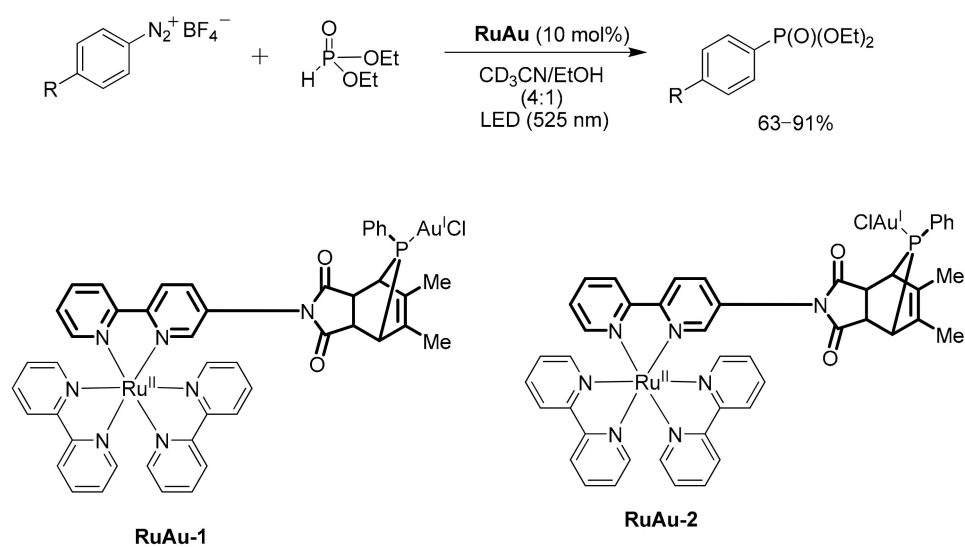
Scheme 22. Arylation of diethylphosphite with diazonium salts catalyzed by heterobimetallic Ru-Au complexes.
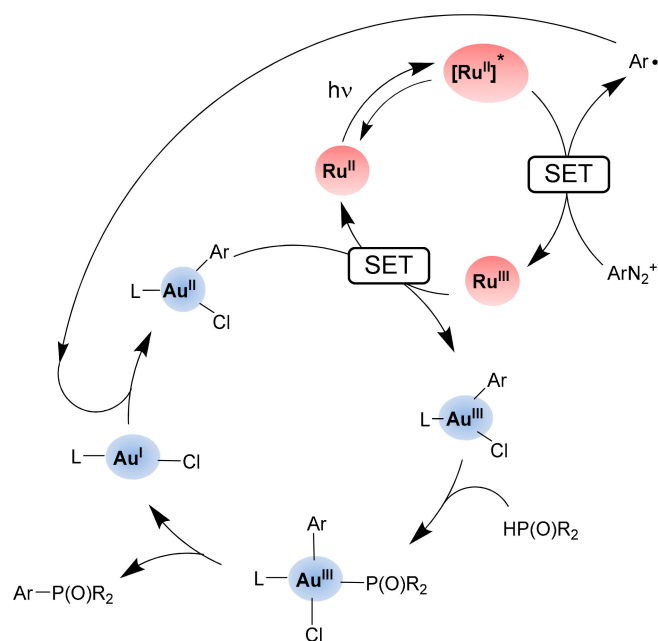
Scheme 23. Proposed mechanism of metallaphotoredox-catalyzed arylation of phosphites with diazonium salts.

The product was formed in all cases when the Au complex was present in the reaction mixture, the yield of the aryl phosphonate ranged from 33 to 64% due to an easy diazonium salt reduction into corresponding aryl radical. Nevertheless, the best yield (74%) was obtained under irradiation in the presence of **RuAu-2** binuclear complex.

3. Conclusions and Prospect

This review covers the application of heterobinuclear complexes as photocatalysts in various reactions. Numerous investigations carried out up to date demonstrate that the covalent binding via the bridging ligand of the photoactive polypyridine complex of Ru(II) or Ir(III) with the catalytically active metal complex favors photoinduced electron or energy transfer between these two parts of the catalytic system. Thus, various heterobinuclear complexes were shown to be efficient for the photocatalytic reduction of CO_2 and hydrogen photogeneration. Variations in the bridging ligand properties, such as

flexibility, π-conjugation, and distance between two metal centers open way to improve these photocatalytic processes. During the last 10 years, metallaphotoredox catalysis, which combines catalysis by transition metal complexes and photoredox catalysis, was extensively developed. Now a great number of catalytic reactions of this type have been introduced to organic synthesis employing catalysts featuring the complexes of copper, nickel, gold, manganese, palladium, and other transition metals. The results discussed in this review demonstrate that the concept of covalent binding of the photoactive complex and metal catalytic center widely studied in H_2 generation and CO_2 reduction processes also can be successfully applied to organic synthesis as it substantially increase the catalyst efficiency and selectivity compared with mixed catalytic systems. However, the mechanisms of these catalytic transformations are not thoroughly studied and are yet to be elucidated. One may confidently state that further introduction of heterobinuclear photocatalysts in the area of metallaphotoredox catalysis on a wider scale will open new vistas for various reactions driven by visible light.

Author Contributions: Conceptualization, A.S.A. and I.P.B.; writing—original draft preparation, V.A.I. and A.S.A.; writing—review and editing, A.S.A., A.D.A. and I.P.B.; funding acquisition, A.S.A. and I.P.B. All authors have read and agreed to the published version of the manuscript.

Conflicts of Interest: The authors declare no conflict of interest.

References

1. Yoon, T.P. Visible light photocatalysis: The development of photocatalytic radical ion cycloadditions. *ACS Catal.* **2013**, *3*, 895–902. [CrossRef] [PubMed]
2. Ravelli, D.; Protti, S.; Fagnoni, M. Carbon–Carbon bond forming reactions via photogenerated intermediates. *Chem. Rev.* **2016**, *116*, 9850–9913. [CrossRef] [PubMed]
3. Ischay, M.A.; Anzovino, M.E.; Du, J.; Yoon, T.P. Efficient visible light photocatalysis of [2+2] enone cycloadditions. *J. Am. Chem. Soc.* **2008**, *130*, 12886–12887. [CrossRef] [PubMed]
4. Nicewicz, D.A.; MacMillan, D.W.C. Merging photoredox catalysis with organocatalysis: The direct asymmetric alkylation of aldehydes. *Science* **2008**, *322*, 77–80. [CrossRef]
5. Corrigan, N.; Shanmugam, S.; Xu, J.; Boyer, C. Photocatalysis in organic and polymer synthesis. *Chem. Soc. Rev.* **2016**, *45*, 6165–6212. [CrossRef]
6. Romero, N.A.; Nicewicz, D.A. Organic photoredox catalysis. *Chem. Rev.* **2016**, *116*, 10075–10166. [CrossRef]
7. Prier, C.K.; Rankic, D.A.; MacMillan, D.W.C. Visible light photoredox catalysis with transition metal complexes: Applications in organic synthesis. *Chem. Rev.* **2013**, *113*, 5322–5363. [CrossRef]
8. Lang, X.; Zhao, J.; Chen, X. Cooperative photoredox catalysis. *Chem. Soc. Rev.* **2016**, *45*, 3026–3038. [CrossRef]
9. Chan, A.Y.; Perry, I.B.; Bissonnette, N.B.; Buksh, B.F.; Edwards, G.A.; Frye, L.I.; Garry, O.L.; Lavagnino, M.N.; Li, B.X.; Liang, Y.; et al. Metallaphotoredox: The merger of photoredox and transition metal catalysis. *Chem. Rev.* **2022**, *122*, 1485–1542. [CrossRef]
10. Lipp, A.; Badir, S.O.; Molander, G.A. Stereoinduction in metallaphotoredox catalysis. *Angew. Chem. Int. Ed.* **2021**, *60*, 1714–1726. [CrossRef]
11. Zhu, C.; Yue, H.; Jia, J.; Rueping, M. Nickel-catalyzed C-Heteroatom cross-coupling reactions under mild conditions via facilitated reductive elimination. *Angew. Chem. Int. Ed.* **2021**, *60*, 17810–17831. [CrossRef] [PubMed]
12. Cheung, K.P.S.; Sarkar, S.; Gevorgyan, V. Visible light-induced transition metal catalysis. *Chem. Rev.* **2022**, *122*, 1543–1625. [CrossRef] [PubMed]
13. Tucker, J.W.; Stephenson, C.R.J. Shining light on photoredox catalysis: Theory and synthetic applications. *J. Org. Chem.* **2012**, *77*, 1617–1622. [CrossRef] [PubMed]
14. Tarantino, G.; Hammond, C. Catalytic formation of $C(sp^3)$–F bonds via heterogeneous photocatalysis. *ACS Catal.* **2018**, *8*, 10321–10330. [CrossRef]
15. Zhang, F.; Wang, X.; Liu, H.; Liu, C.; Wan, Y.; Long, Y.; Cai, Z. Recent advances and applications of semiconductor photocatalytic technology. *Appl. Sci.* **2019**, *9*, 2489. [CrossRef]
16. Lang, X.; Chen, X.; Zhao, J. Heterogeneous visible light photocatalysis for selective organic transformations. *Chem. Soc. Rev.* **2014**, *43*, 473–486. [CrossRef]
17. Chen, J.; Cen, J.; Xu, X.; Li, X. The application of heterogeneous visible light photocatalysts in organic synthesis. *Catal. Sci. Technol.* **2016**, *6*, 349–362. [CrossRef]
18. Pieber, B.; Shalom, M.; Antonietti, M.; Seeberger, P.H.; Gilmore, K. Continuous heterogeneous photocatalysis in serial micro-batch reactors. *Angew. Chem. Int. Ed.* **2018**, *57*, 9976–9979. [CrossRef]

19. Dong, K.; Pezzetta, C.; Chen, Q.-C.; Kaushansky, A.; Agosti, A.; Bergamini, G.; Davidson, R.; Amirav, L. Nanorod photocatalysts for C−O cross-coupling reactions. *ChemCatChem* **2022**, *14*, e202200477. [CrossRef]

20. Easun, T.L.; Alsindi, W.Z.; Towrie, M.; Ronayne, K.L.; Sun, X.-Z.; Ward, M.D.; George, M.W. Photoinduced energy transfer in a conformationally flexible Re(I)/Ru(II) dyad probed by time-resolved infrared spectroscopy: Effects of Conformation and Spatial Localization of Excited States. *Inorg. Chem.* **2008**, *47*, 5071–5078. [CrossRef]

21. Schallenberg, D.; Neubauer, A.; Erdmann, E.; Tänzler, M.; Villinger, A.; Lochbrunner, S.; Seidel, W.W. Dinuclear Ru/Ni, Ir/Ni, and Ir/Pt complexes with bridging phenanthroline-5,6-dithiolate: Synthesis, structure, and electrochemical and photophysical Behavior. *Inorg. Chem.* **2014**, *53*, 8859–8873. [CrossRef] [PubMed]

22. Troian-Gautier, L.; Moucheron, C. Ruthenium^{II} complexes bearing fused polycyclic ligands: From fundamental aspects to potential applications. *Molecules* **2014**, *19*, 5028–5087. [CrossRef] [PubMed]

23. Cho, Y.-J.; Kim, S.-Y.; Choi, C.M.; Kim, N.J.; Kim, C.H.; Cho, D.W.; Son, H.-J.; Pac, C.; Kang, S.O. Photophysics and excited-state properties of cyclometalated iridium(III)–platinum(II) and iridium(III)–iridium(III) bimetallic complexes bridged by dipyridylpyrazine. *Inorg. Chem.* **2017**, *56*, 5305–5315. [CrossRef] [PubMed]

24. Laramée-Milette, B.; Hanan, G.S. Going against the flow: Os(II)-to-Ru(II) energy transfer in rod-like polypyridyl chromophore. *Chem. Commun.* **2017**, *53*, 10496–10499. [CrossRef] [PubMed]

25. Zigler, D.F.; Morseth, Z.A.; White, T.A.; Canterbury, T.R.; Sayre, H.J.; Rodríguez-Corrales, J.Á.; Brennaman, M.K.; Brewer, K.J.; Papanikolas, J.M. Ultrafast kinetics of supramolecules with a Ru(II)- or Os(II)-polypyridyl light absorber, *cis*-Rh(III)Cl$_2$-polypyridyl electron collector, and 2,3-bis(2-pyridyl)pyrazine bridge. *Inorg. Chim. Acta* **2017**, *454*, 266–274. [CrossRef]

26. Erdmann, E.; Lütgens, M.; Lochbrunner, S.; Seidel, W.W. Ultrafast energy transfer in dinuclear complexes with bridging 1,10-phenanthroline-5,6-dithiolate. *Inorg. Chem.* **2018**, *57*, 4849–4863. [CrossRef]

27. Staniszewska, M.; Kupfer, S.; Guthmuller, J. Effect of the catalytic center on the electron transfer dynamics in hydrogen-evolving ruthenium-based photocatalysts investigated by theoretical calculations. *J. Phys. Chem. C* **2019**, *123*, 16003–16013. [CrossRef]

28. Zedler, L.; Müller, C.; Wintergerst, P.; Mengele, A.K.; Rau, S.; Dietzek-Ivanšić, B. Influence of the linker chemistry on the photoinduced charge-transfer dynamics of hetero-dinuclear photocatalysts. *Chem. Eur. J.* **2022**, *28*, e202200490. [CrossRef]

29. Tamaki, Y.; Ishitani, O. Supramolecular photocatalysts for the reduction of CO$_2$. *ACS Catalysis* **2017**, *7*, 3394–3409. [CrossRef]

30. Kuramochi, Y.; Ishitani, O.; Ishida, H. Reaction mechanisms of catalytic photochemical CO$_2$ reduction using Re(I) and Ru(II) complexes. *Coord. Chem. Rev.* **2018**, *373*, 333–356. [CrossRef]

31. Pirzada, B.M.; Dar, A.H.; Shaikh, M.N.; Qurashi, A. Reticular-chemistry-inspired supramolecule design as a tool to achieve efficient photocatalysts for CO$_2$ reduction. *ACS Omega* **2021**, *6*, 29291–29324. [CrossRef]

32. Halpin, Y.; Pryce, M.T.; Rau, S.; Dini, D.; Vos, J.G. Recent progress in the development of bimetallic photocatalysts for hydrogen generation. *Dalton Trans.* **2013**, *42*, 16243–16254. [CrossRef] [PubMed]

33. Manbeck, G.F.; Brewer, K.J. Photoinitiated electron collection in polyazine chromophores coupled to water reduction catalysts for solar H$_2$ production. *Coord. Chem. Rev.* **2013**, *257*, 1660–1675. [CrossRef]

34. Dini, D.; Pryce, M.T.; Schulz, M.; Vos, J.G. CHAPTER 12 Metallosupramolecular assemblies for application as photocatalysts for the production of solar fuels. In *Functional Metallosupramolecular Materials*; The Royal Society of Chemistry: London, UK, 2015; pp. 345–396.

35. Juris, A.; Balzani, V.; Barigelletti, F.; Campagna, S.; Belser, P.; von Zelewsky, A. Ru(II) polypyridine complexes: Photophysics, photochemistry, eletrochemistry, and chemiluminescence. *Coord. Chem. Rev.* **1988**, *84*, 85–277. [CrossRef]

36. Lutz, F.; Lorenzo-Parodi, N.; Schmidt, T.C.; Niemeyer, J. Heteroternary cucurbit [8] uril complexes as supramolecular scaffolds for self-assembled bifunctional photoredoxcatalysts. *Chem. Commun.* **2021**, *57*, 2887–2890. [CrossRef]

37. Frischmann, P.D.; Mahata, K.; Würthner, F. Powering the future of molecular artificial photosynthesis with light-harvesting metallosupramolecular dye assemblies. *Chem. Soc. Rev.* **2013**, *42*, 1847–1870. [CrossRef]

38. Bindra, G.S.; Schulz, M.; Paul, A.; Soman, S.; Groarke, R.; Inglis, J.; Pryce, M.T.; Browne, W.R.; Rau, S.; Maclean, B.J.; et al. The effect of peripheral bipyridine ligands on the photocatalytic hydrogen production activity of Ru/Pd catalysts. *Dalton Trans.* **2011**, *40*, 10812–10814. [CrossRef]

39. Bindra, G.S.; Schulz, M.; Paul, A.; Groarke, R.; Soman, S.; Inglis, J.L.; Browne, W.R.; Pfeffer, M.G.; Rau, S.; MacLean, B.J.; et al. The role of bridging ligand in hydrogen generation by photocatalytic Ru/Pd assemblies. *Dalton Trans.* **2012**, *41*, 13050–13059. [CrossRef]

40. Kowacs, T.; O'Reilly, L.; Pan, Q.; Huijser, A.; Lang, P.; Rau, S.; Browne, W.R.; Pryce, M.T.; Vos, J.G. Subtle changes to peripheral ligands enable high turnover numbers for photocatalytic hydrogen generation with supramolecular photocatalysts. *Inorg. Chem.* **2016**, *55*, 2685–2690. [CrossRef]

41. Pan, Q.; Mecozzi, F.; Korterik, J.P.; Vos, J.G.; Browne, W.R.; Huijser, A. The critical role played by the catalytic moiety in the early-time photodynamics of hydrogen-generating bimetallic photocatalysts. *ChemPhysChem* **2016**, *17*, 2654–2659. [CrossRef]

42. Kowacs, T.; Pan, Q.; Lang, P.; O'Reilly, L.; Rau, S.; Browne, W.R.; Pryce, M.T.; Huijser, A.; Vos, J.G. Supramolecular bimetallic assemblies for photocatalytic hydrogen generation from water. *Faraday Discuss.* **2015**, *185*, 143–170. [CrossRef] [PubMed]

43. Zhou, R.; Manbeck, G.F.; Wimer, D.G.; Brewer, K.J. A new Ru^{II}Rh^{III} bimetallic with a single Rh–Cl bond as a supramolecular photocatalyst for proton reduction. *Chem. Commun.* **2015**, *51*, 12966–12969. [CrossRef] [PubMed]

44. Rogers, H.M.; Arachchige, S.M.; Brewer, K.J. Enhancement of solar fuel production schemes by using a Ru,Rh,Ru supramolecular photocatalyst containing hydroxide labile ligands. *Chem. Eur. J.* **2015**, *21*, 16948–16954. [CrossRef] [PubMed]

45. Canterbury, T.R.; Arachchige, S.M.; Brewer, K.J.; Moore, R.B. A new hydrophilic supramolecular photocatalyst for the production of H_2 in aerobic aqueous solutions. *Chem. Commun.* **2016**, *52*, 8663–8666. [CrossRef]

46. White, J.K.; Brewer, K.J. A new Ru,Ru,Pt supramolecular architecture for photocatalytic H_2 production. *Chem. Commun.* **2015**, *51*, 16123–16126. [CrossRef] [PubMed]

47. Karnahl, M.; Kuhnt, C.; Ma, F.; Yartsev, A.; Schmitt, M.; Dietzek, B.; Rau, S.; Popp, J. Tuning of photocatalytic hydrogen production and photoinduced intramolecular electron transfer rates by regioselective bridging ligand substitution. *ChemPhysChem* **2011**, *12*, 2101–2109. [CrossRef]

48. Pfeffer, M.G.; Kowacs, T.; Wächtler, M.; Guthmuller, J.; Dietzek, B.; Vos, J.G.; Rau, S. Optimization of hydrogen-evolving photochemical molecular devices. *Angew. Chem. Int. Ed.* **2015**, *54*, 6627–6631. [CrossRef]

49. Pfeffer, M.G.; Schäfer, B.; Smolentsev, G.; Uhlig, J.; Nazarenko, E.; Guthmuller, J.; Kuhnt, C.; Wächtler, M.; Dietzek, B.; Sundström, V.; et al. Palladium versus platinum: The metal in the catalytic center of a molecular photocatalyst determines the mechanism of the hydrogen production with visible light. *Angew. Chem. Int. Ed.* **2015**, *54*, 5044–5048. [CrossRef]

50. Mengele, A.K.; Kaufhold, S.; Streb, C.; Rau, S. Generation of a stable supramolecular hydrogen evolving photocatalyst by alteration of the catalytic center. *Dalton Trans.* **2016**, *45*, 6612–6618. [CrossRef]

51. Pfeffer, M.G.; Zedler, L.; Kupfer, S.; Paul, M.; Schwalbe, M.; Peuntinger, K.; Guldi, D.M.; Guthmuller, J.; Popp, J.; Gräfe, S.; et al. Tuning of photocatalytic activity by creating a tridentate coordination sphere for palladium. *Dalton Trans.* **2014**, *43*, 11676–11686. [CrossRef]

52. Kaufhold, S.; Imanbaew, D.; Riehn, C.; Rau, S. Rational in situ tuning of a supramolecular photocatalyst for hydrogen evolution. *Sustain. Energy Fuels* **2017**, *1*, 2066–2070. [CrossRef]

53. Das, N.; Bindra, G.S.; Paul, A.; Vos, J.G.; Schulz, M.; Pryce, M.T. Enhancing photocatalytic hydrogen generation: The impact of the peripheral ligands in Ru/Pd and Ru/Pt complexes. *Chem. Eur. J.* **2017**, *23*, 5330–5337. [CrossRef] [PubMed]

54. Stoll, T.; Gennari, M.; Fortage, J.; Castillo, C.E.; Rebarz, M.; Sliwa, M.; Poizat, O.; Odobel, F.; Deronzier, A.; Collomb, M.-N. An efficient Ru^{II}–Rh^{III}–Ru^{II} polypyridyl photocatalyst for visible-light-driven hydrogen production in aqueous solution. *Angew. Chem. Int. Ed.* **2014**, *53*, 1654–1658. [CrossRef] [PubMed]

55. Lentz, C.; Schott, O.; Auvray, T.; Hanan, G.S.; Elias, B. Design and photophysical studies of iridium(III)–cobalt(III) dyads and their application for dihydrogen photo-evolution. *Dalton Trans.* **2019**, *48*, 15567–15576. [CrossRef]

56. Zedler, L.; Wintergerst, P.; Mengele, A.K.; Müller, C.; Li, C.; Dietzek-Ivanšić, B.; Rau, S. Outpacing conventional nicotinamide hydrogenation catalysis by a strongly communicating heterodinuclear photocatalyst. *Nat. Commun.* **2022**, *13*, 2538. [CrossRef]

57. Kimura, E.; Wada, S.; Shionoya, M.; Takahashi, T.; Litaka, Y. A novel cyclam–nickel(II) complex appended with a tris-(2,2′-bipyridine) ruthenium(II) complex (cyclam = 1,4,8,11-tetra-azacyclotetradecane). *J. Chem. Soc. Chem. Commun.* **1990**, *5*, 397–398. [CrossRef]

58. Kimura, E.; Bu, X.; Shionoya, M.; Wada, S.; Maruyama, S. A new nickel(II) cyclam (cyclam = 1,4,8,11-tetraazacyclotetradecane) complex covalently attached to tris(1,10-phenanthroline)ruthenium(2+). A new candidate for the catalytic photoreduction of carbon dioxide. *Inorg. Chem.* **1992**, *31*, 4542–4546. [CrossRef]

59. Kimura, E.; Wada, S.; Shionoya, M.; Okazaki, Y. New series of multifunctionalized nickel(II)-cyclam (cyclam = 1,4,8,11-tetraazacyclotetradecane) complexes. application to the photoreduction of carbon dioxide. *Inorg. Chem.* **1994**, *33*, 770–778. [CrossRef]

60. Komatsuzaki, N.; Himeda, Y.; Hirose, T.; Sugihara, H.; Kasuga, K. Synthesis and photochemical properties of ruthenium–cobalt and ruthenium–nickel dinuclear complexes. *Bull. Chem. Soc. Jpn.* **1999**, *72*, 725–731. [CrossRef]

61. Gholamkhass, B.; Mametsuka, H.; Koike, K.; Tanabe, T.; Furue, M.; Ishitani, O. Architecture of supramolecular metal complexes for photocatalytic CO_2 reduction: ruthenium−rhenium bi- and tetranuclear complexes. *Inorg. Chem.* **2005**, *44*, 2326–2336. [CrossRef]

62. Koike, K.; Naito, S.; Sato, S.; Tamaki, Y.; Ishitani, O. Architecture of supramolecular metal complexes for photocatalytic CO_2 reduction: III: Effects of length of alkyl chain connecting photosensitizer to catalyst. *J. Photochem. Photobiol. A Chem.* **2009**, *207*, 109–114. [CrossRef]

63. Bian, Z.-Y.; Chi, S.-M.; Li, L.; Fu, W. Conjugation effect of the bridging ligand on the CO_2 reduction properties in difunctional photocatalysts. *Dalton Trans.* **2010**, *39*, 7884–7887. [CrossRef] [PubMed]

64. Tamaki, Y.; Koike, K.; Morimoto, T.; Ishitani, O. Substantial improvement in the efficiency and durability of a photocatalyst for carbon dioxide reduction using a benzoimidazole derivative as an electron donor. *J. Catal.* **2013**, *304*, 22–28. [CrossRef]

65. Kato, E.; Takeda, H.; Koike, K.; Ohkubo, K.; Ishitani, O. Ru(II)–Re(I) binuclear photocatalysts connected by –CH_2XCH_2– (X = O, S, CH_2) for CO_2 reduction. *Chem. Sci.* **2015**, *6*, 3003–3012. [CrossRef]

66. Yamazaki, Y.; Ohkubo, K.; Saito, D.; Yatsu, T.; Tamaki, Y.; Tanaka, S.I.; Koike, K.; Onda, K.; Ishitani, O. Kinetics and mechanism of intramolecular electron transfer in Ru(II)–Re(I) supramolecular CO_2–reduction photocatalysts: Effects of bridging ligands. *Inorg. Chem.* **2019**, *58*, 11480–11492. [CrossRef]

67. Tamaki, Y.; Watanabe, K.; Koike, K.; Inoue, H.; Morimoto, T.; Ishitani, O. Development of highly efficient supramolecular CO_2 reduction photocatalysts with high turnover frequency and durability. *Faraday Discuss.* **2012**, *155*, 115–127. [CrossRef]

68. Ohkubo, K.; Yamazaki, Y.; Nakashima, T.; Tamaki, Y.; Koike, K.; Ishitani, O. Photocatalyses of Ru(II)–Re(I) binuclear complexes connected through two ethylene chains for CO_2 reduction. *J. Catal.* **2016**, *343*, 278–289. [CrossRef]

69. Brown, C.M.; Auvray, T.; DeLuca, E.E.; Ezhova, M.B.; Hanan, G.S.; Wolf, M.O. Controlling photocatalytic reduction of CO$_2$ in Ru(II)/Re(I) dyads via linker oxidation state. *Chem. Commun.* **2020**, *56*, 10750–10753. [CrossRef]

70. Gotico, P.; Tran, T.-T.; Baron, A.; Vauzeilles, B.; Lefumeux, C.; Ha-Thi, M.-H.; Pino, T.; Halime, Z.; Quaranta, A.; Leibl, W.; et al. Tracking charge accumulation in a functional triazole-linked ruthenium-rhenium dyad towards photocatalytic carbon dioxide reduction. *ChemPhotoChem* **2021**, *5*, 654–664. [CrossRef]

71. Cerpentier, F.J.R.; Karlsson, J.; Lalrempuia, R.; Brandon, M.P.; Sazanovich, I.V.; Greetham, G.M.; Gibson, E.A.; Pryce, M.T. Ruthenium assemblies for CO$_2$ reduction and H$_2$ generation: Time resolved infrared spectroscopy, spectroelectrochemistry and a photocatalysis study in solution and on NiO. *Front. Chem.* **2021**, *9*, 795877. [CrossRef]

72. Kuttassery, F.; Kumagai, H.; Kamata, R.; Ebato, Y.; Higashi, M.; Suzuki, H.; Abe, R.; Ishitani, O. Supramolecular photocatalysts fixed on the inside of the polypyrrole layer in dye sensitized molecular photocathodes: Application to photocatalytic CO$_2$ reduction coupled with water oxidation. *Chem. Sci.* **2021**, *12*, 13216–13232. [CrossRef] [PubMed]

73. Maier, A.S.; Thomas, C.; Kränzlein, M.; Pehl, T.M.; Rieger, B. Macromolecular rhenium–ruthenium complexes for photocatalytic CO$_2$ conversion: From catalytic Lewis pair polymerization to well-defined poly(vinyl bipyridine)–metal complexes. *Macromolecules* **2022**, *55*, 7039–7048. [CrossRef]

74. Fabry, D.C.; Koizumi, H.; Ghosh, D.; Yamazaki, Y.; Takeda, H.; Tamaki, Y.; Ishitani, O. A Ru(II)–Mn(I) supramolecular photocatalyst for CO$_2$ reduction. *Organometallics* **2020**, *39*, 1511–1518. [CrossRef]

75. Kitagawa, Y.; Takeda, H.; Ohashi, K.; Asatani, T.; Kosumi, D.; Hashimoto, H.; Ishitani, O.; Tamiaki, H. Photochemical reduction of CO$_2$ with red light using synthetic chlorophyll–rhenium bipyridine dyad. *Chem. Lett.* **2014**, *43*, 1383–1385. [CrossRef]

76. Kuramochi, Y.; Fujisawa, Y.; Satake, A. Photocatalytic CO$_2$ reduction mediated by electron transfer via the excited triplet state of Zn(II) porphyrin. *J. Am. Chem. Soc.* **2020**, *142*, 705–709. [CrossRef]

77. Kuramochi, Y.; Satake, A. Photocatalytic CO$_2$ reductions catalyzed by meso-(1,10-phenanthrolin-2-yl)-porphyrins having a rhenium(I) tricarbonyl complex. *Chem. Eur. J.* **2020**, *26*, 16365–16373. [CrossRef]

78. Lang, P.; Pfrunder, M.; Quach, G.; Braun-Cula, B.; Moore, E.G.; Schwalbe, M. Sensitized photochemical CO$_2$ reduction by hetero-Pacman compounds linking a Re^I tricarbonyl with a porphyrin unit. *Chem. Eur. J.* **2019**, *25*, 4509–4519. [CrossRef] [PubMed]

79. Matlachowski, C.; Braun, B.; Tschierlei, S.; Schwalbe, M. Photochemical CO$_2$ reduction catalyzed by phenanthroline extended tetramesityl porphyrin complexes linked with a rhenium(I) tricarbonyl unit. *Inorg. Chem.* **2015**, *54*, 10351–10360. [CrossRef]

80. Schneider, J.; Vuong, K.Q.; Calladine, J.A.; Sun, X.-Z.; Whitwood, A.C.; George, M.W.; Perutz, R.N. Photochemistry and photophysics of a Pd(II) metalloporphyrin: Re(I) tricarbonyl bipyridine molecular dyad and its activity toward the photoreduction of CO$_2$ to CO. *Inorg. Chem.* **2011**, *50*, 11877–11889. [CrossRef] [PubMed]

81. Windle, C.D.; Câmpian, M.V.; Duhme-Klair, A.-K.; Gibson, E.A.; Perutz, R.N.; Schneider, J. CO$_2$ photoreduction with long-wavelength light: Dyads and monomers of zinc porphyrin and rhenium bipyridine. *Chem. Commun.* **2012**, *48*, 8189–8191. [CrossRef]

82. Windle, C.D.; George, M.W.; Perutz, R.N.; Summers, P.A.; Sun, X.Z.; Whitwood, A.C. Comparison of rhenium–porphyrin dyads for CO$_2$ photoreduction: Photocatalytic studies and charge separation dynamics studied by time-resolved IR spectroscopy. *Chem. Sci.* **2015**, *6*, 6847–6864. [CrossRef] [PubMed]

83. Inagaki, A.; Edure, S.; Yatsuda, S.; Akita, M. Highly selective photo-catalytic dimerization of α-methylstyrene by a novel palladium complex with photosensitizing ruthenium(II) polypyridyl moiety. *Chem. Commun.* **2005**, *43*, 5468–5470. [CrossRef] [PubMed]

84. Inagaki, A.; Yatsuda, S.; Edure, S.; Suzuki, A.; Takahashi, T.; Akita, M. Synthesis of Pd complexes combined with photosensitizing of a ruthenium(II) polypyridyl moiety through a series of substituted bipyrimidine bridges. Substituent effect of the bridging ligand on the photocatalytic dimerization of α-methylstyrene. *Inorg. Chem.* **2007**, *46*, 2432–2445. [CrossRef] [PubMed]

85. Nitadori, H.; Takahashi, T.; Inagaki, A.; Akita, M. Enhanced photocatalytic activity of α-methylstyrene oligomerization through effective metal-to-ligand charge-transfer localization on the bridging ligand. *Inorg. Chem.* **2012**, *51*, 51–62. [CrossRef] [PubMed]

86. Murata, K.; Araki, M.; Inagaki, A.; Akita, M. Syntheses, photophysical properties, and reactivities of novel bichromophoric Pd complexes composed of Ru(II)–polypyridyl and naphthyl moieties. *Dalton Trans.* **2013**, *42*, 6989–7001. [CrossRef] [PubMed]

87. Murata, K.; Inagaki, A.; Akita, M.; Halet, J.-F.; Costuas, K. Revelation of the photoactive species in the photocatalytic dimerization of α-methylstyrene by a dinuclear ruthenium–palladium complex. *Inorg. Chem.* **2013**, *52*, 8030–8039. [CrossRef]

88. Kikuchi, S.; Saito, K.; Akita, M.; Inagaki, A. Nonradical light-controlled polymerization of styrene and vinyl ethers catalyzed by an iridium-palladium photocatalyst. *Organometallics* **2018**, *37*, 359–366. [CrossRef]

89. Fujiwara, T.; Nomura, K.; Inagaki, A. Cu–Pd dinuclear complexes with earth-abundant Cu photosensitizer: Synthesis and photopolymerization. *Organometallics* **2020**, *39*, 2464–2469. [CrossRef]

90. Armaroli, N. Photoactive mono- and polynuclear Cu(I)–phenanthrolines. A viable alternative to Ru(II)–polypyridines? *Chem. Soc. Rev.* **2001**, *30*, 113–124. [CrossRef]

91. Nicolaou, K.C.; Bulger, P.G.; Sarlah, D. Palladium-catalyzed cross-coupling reactions in total synthesis. *Angew. Chem. Int. Ed.* **2005**, *44*, 4442–4489. [CrossRef]

92. Buchwald, S.L. Cross coupling. *Acc. Chem. Res.* **2008**, *41*, 1439. [CrossRef] [PubMed]

93. Johansson Seechurn, C.C.; Kitching, M.O.; Colacot, T.J.; Snieckus, V. Palladium-Catalyzed cross-coupling: A historical contextual perspective to the 2010 Nobel prize. *Angew. Chem. Int. Ed.* **2012**, *51*, 5062–5085. [CrossRef] [PubMed]

94. Devendar, P.; Qu, R.-Y.; Kang, W.-M.; He, B.; Yang, G.-F. Palladium-Catalyzed Cross-Coupling Reactions: A Powerful Tool for the Synthesis of Agrochemicals. *J. Agric. Food. Chem.* **2018**, *66*, 8914–8934. [CrossRef] [PubMed]

95. Osawa, M.; Nagai, H.; Akita, M. Photo-activation of Pd-catalyzed Sonogashira coupling using a Ru/bipyridine complex as energy transfer agent. *Dalton Trans.* **2007**, *8*, 827–829. [CrossRef] [PubMed]

96. Dissanayake, K.C.; Ebukuyo, P.O.; Dhahir, Y.J.; Wheeler, K.; He, H. A BODIPY-functionalized Pd^{II} photoredox catalyst for Sonogashira C–C cross-coupling reactions. *Chem. Commun.* **2019**, *55*, 4973–4976. [CrossRef] [PubMed]

97. Mori, K.; Kawashima, M.; Yamashita, H. Visible-light-enhanced Suzuki–Miyaura coupling reaction by cooperative photocatalysis with an Ru–Pd bimetallic complex. *Chem. Commun.* **2014**, *50*, 14501–14503. [CrossRef]

98. Yao, S.Y.; Cao, M.L.; Zhang, X.L. Photoaccelerated energy transfer catalysis of the Suzuki-Miyaura coupling through ligand regulation on Ir(III)-Pd(II) bimetallic complexes. *RSC Adv.* **2020**, *10*, 42874–42882. [CrossRef] [PubMed]

99. Yang, C.-H.; Liu, Y.-H.; Peng, S.-M.; Liu, S.-T. Photoaccelerated Suzuki–Miyaura and Sonogashira coupling reactions catalyzed by an Ir-Pd binuclear complex. *Mol. Catal.* **2022**, *522*, 112232. [CrossRef]

100. Li, M.; Chia, X.L.; Zhu, Y. Tethered photocatalyst-directed palladium-catalysed C–H allenylation of *N*-aryl tetrahydroisoquinolines. *Chem. Commun.* **2022**, *58*, 4719–4722. [CrossRef]

101. Herrero, C.; Quaranta, A.; Fallahpour, R.-A.; Leibl, W.; Aukauloo, A. Identification of the Different Mechanisms of Activation of a [Ru^{II}(tpy)(bpy)(OH$_2$)]$^{2+}$ Catalyst by Modified Ruthenium Sensitizers in Supramolecular Complexes. *J. Phys. Chem. C* **2013**, *117*, 9605–9612. [CrossRef]

102. Herrero, C.; Quaranta, A.; Leibl, W.; Rutherford, A.W.; Aukauloo, A. Artificial photosynthetic systems. Using light and water to provide electrons and protons for the synthesis of a fuel. *Energy Environ. Sci.* **2011**, *4*, 2353–2365. [CrossRef]

103. Nikoloudakis, E.; Alsaleh, A.Z.; Charalambidis, G.; Coutsolelos, A.G.; D'Souza, F. A covalently linked nickel(II) porphyrin–ruthenium(II) tris(bipyridyl) dyad for efficient photocatalytic water oxidation. *Chem. Commun.* **2022**, *58*, 12078–12081. [CrossRef] [PubMed]

104. Chao, D.; Fu, W.-F. Insight into highly selective photocatalytic oxidation of alcohols by a new trinuclear ruthenium complex with visible light. *Dalton Trans.* **2014**, *43*, 306–310. [CrossRef] [PubMed]

105. Herrero, C.; Quaranta, A.; Sircoglou, M.; Sénéchal-David, K.; Baron, A.; Marín, I.M.; Buron, C.; Baltaze, J.-P.; Leibl, W.; Aukauloo, A.; et al. Successive light-induced two electron transfers in a Ru–Fe supramolecular assembly: From Ru–Fe(II)–OH$_2$ to Ru–Fe(IV)–oxo. *Chem. Sci.* **2015**, *6*, 2323–2327. [CrossRef]

106. Skolia, E.; Gkizis, P.L.; Kokotos, C.G. Aerobic photocatalysis: Oxidation of sulfides to sulfoxides. *ChemPlusChem* **2022**, *87*, e202200008. [CrossRef]

107. Baciocchi, E.; Giacco, T.D.; Elisei, F.; Gerini, M.F.; Guerra, M.; Lapi, A.; Liberali, P. Electron transfer and singlet oxygen mechanisms in the photooxygenation of dibutyl sulfide and thioanisole in MeCN Sensitized by *N*-methylquinolinium tetrafluoborate and 9,10-dicyanoanthracene. The probable involvement of a thiadioxirane intermediate in electron transfer photooxygenations. *J. Am. Chem. Soc.* **2003**, *125*, 16444–16454. [CrossRef]

108. Clennan, E.L. Persulfoxide: Key intermediate in reactions of singlet oxygen with sulfides. *Acc. Chem. Res.* **2001**, *34*, 875–884. [CrossRef]

109. Iali, W.; Lanoe, P.-H.; Torelli, S.; Jouvenot, D.; Loiseau, F.; Lebrun, C.; Hamelin, O.; Ménage, S. A ruthenium(II)–copper(II) dyad for the photocatalytic oxygenation of organic substrates mediated by dioxygen activation. *Angew. Chem. Int. Ed.* **2015**, *54*, 8415–8419. [CrossRef]

110. Chao, D.; Zhao, M. Robust Cooperative photo-oxidation of sulfides without sacrificial reagent under air using a dinuclear Ru^{II}–Cu^{II} assembly. *ChemSusChem* **2017**, *10*, 3358–3362. [CrossRef]

111. Ananikov, V.P. Nickel: The "spirited horse" of transition metal catalysis. *ACS Catal.* **2015**, *5*, 1964–1971. [CrossRef]

112. Thoke, M.B.; Sun, G.-J.; Borse, R.A.; Lin, P.; Lin, S.-X. Unimolecular cooperative metallaphotocatalysis with conjugately bridged Ir–Ni complexes and its applications in organic coupling reactions. *Org. Chem. Front.* **2022**, *9*, 1797–1807. [CrossRef]

113. Kumar, P.; Joshi, C.; Srivastava, A.K.; Gupta, P.; Boukherroub, R.; Jain, S.L. Visible light assisted photocatalytic [3+2] azide–alkyne "Click" reaction for the synthesis of 1,4-substituted 1,2,3-triazoles using a novel bimetallic Ru–Mn complex. *ACS Sustain. Chem. Eng.* **2016**, *4*, 69–75. [CrossRef]

114. Bayer, L.; Birenheide, B.S.; Krämer, F.; Lebedkin, S.; Breher, F. Heterobimetallic gold/ruthenium complexes synthesized via post-functionalization and applied in dual photoredox gold catalysis. *Chem. Eur. J.* **2022**, *28*, e202201856. [CrossRef] [PubMed]